JOURNAL OF MAGNETIC RESONANCE **135,** 380–405 (1998)
ARTICLE NO. MN981591

A Mathematical Assessment of the Precision of Parameters in Measuring Resonance Spectra

Elke M. Golding*,[1] and Raymund M. Golding†

**Department of Neurosurgery, Baylor College of Medicine, Houston, Texas 77030; and †National Unit for Multidisciplinary Studies of Spinal Pain, Townsville General Hospital, P.O. Box 670, Townsville, Queensland 4810, Australia*

E-mail: egolding@bcm.tmc.edu

Received September 23, 1997; revised August 21, 1998

The accurate interpretation of *in vivo* magnetic resonance spectroscopy (MRS) spectra requires a complete understanding of the associated noise-induced errors. In this paper, we address the effect of complex correlated noise patterns on the measurement of a set of *peak* parameters. This is examined initially at the level of a single spectral analysis followed by addressing the noise-induced errors associated with determining the *signal* parameters from the *peak* parameters. We describe a relatively simple method for calculating these errors for any correlated noise pattern in terms of the noise standard deviation and correlation length. The results are presented in such a way that an estimate of the errors may be made from a single MRS spectrum. We also explore how, under certain circumstances, the lineshape of the signal may be determined. We then apply these results to reexamine a set of *in vivo* ^{31}P MRS spectra obtained from rat brain prior to and following moderate fluid percussion injury. The approach outlined in this paper will demonstrate how meaningful results may be obtained from spectra where the signal-to-noise ratio (SNR) is quite small and where knowledge of the precise shape of the signal and the detail of the noise pattern is unknown. In essence, we show how to determine the expected errors in the spectral parameters from an estimate of the SNR from a single spectrum, thereby allowing a more discriminative interpretation of the data. © 1998 Academic Press

Key Words: **correlation length; correlated noise; errors; magnetic resonance spectroscopy; signal; standard deviations; traumatic head injury.**

INTRODUCTION

The application of phosphorus magnetic resonance spectroscopy (^{31}P MRS) to the study of metabolism and bioenergetics *in vivo* has grown steadily over the past two decades. The enticement of using ^{31}P MRS over conventional metabolic analyses arises from its non-invasive and non-destructive nature, which permits continuous spectra to be obtained from a single organ or tissue in real-time. Routinely, free intracellular magnesium concentration (free [Mg^{2+}]) and intracellular pH are calculated from chemical shift assignments, and the ratio of energy metabolites PCr, ATP, and P_i calculated from area analysis (*1*).

As with any scientific technique however, ^{31}P MRS has strengths and limitations. If these strengths and limitations are not fully appreciated by MRS users, problems may arise with respect to quantification and subsequent interpretation of results concerning a particular physiological or pathophysiological state. We recently reported (*2*) that the intrinsic errors of typical ^{31}P MRS estimates of free [Mg^{2+}] in rat brain *in vivo* are sufficiently large to cast doubt on the significance of previously published results showing its decline in association with moderate brain injury (*3*). We reached this conclusion by investigating the intrinsic errors associated with chemical shift assignments from *in vivo* ^{31}P MRS spectra. Using simulated spectra over a range of 1.2 ppm, a relationship between the standard deviation of the chemical shift position, $\sigma(m_3)$ and the signal-to-noise ratio (SNR) was derived empirically as described by

$$\sigma(m_3) * \mathrm{SNR} = 0.090. \qquad [1]$$

Although the focus of this paper is on ^{31}P MRS spectra, the results are quite general and may be applied to any form of spectroscopy. Conventionally, effort has been directed towards minimizing noise levels in order to optimize the signal but in some instances, and particularly *in vivo*, the noise levels are higher than acceptable. It is therefore critical to know the limitations of such measurements. In addition, the noise patterns may be quite complex and possess a frequency dependence, in which case we are dealing with correlated noise.

Previous studies examining the accuracy and precision of signal parameter measurements have focused on the errors in determining a specific set of parameters. In particular, Posener (*4*) examined the standard deviation of the height and position of a Gaussian and Lorentzian shaped signal embedded in white or uncorrelated noise. Chen *et al.* (*5*) extended Posener's work to include the linewidth standard deviation. They concluded that the theoretical calculations of the standard deviations were

[1] To whom correspondence should be addressed.

1090-7807/98 $25.00

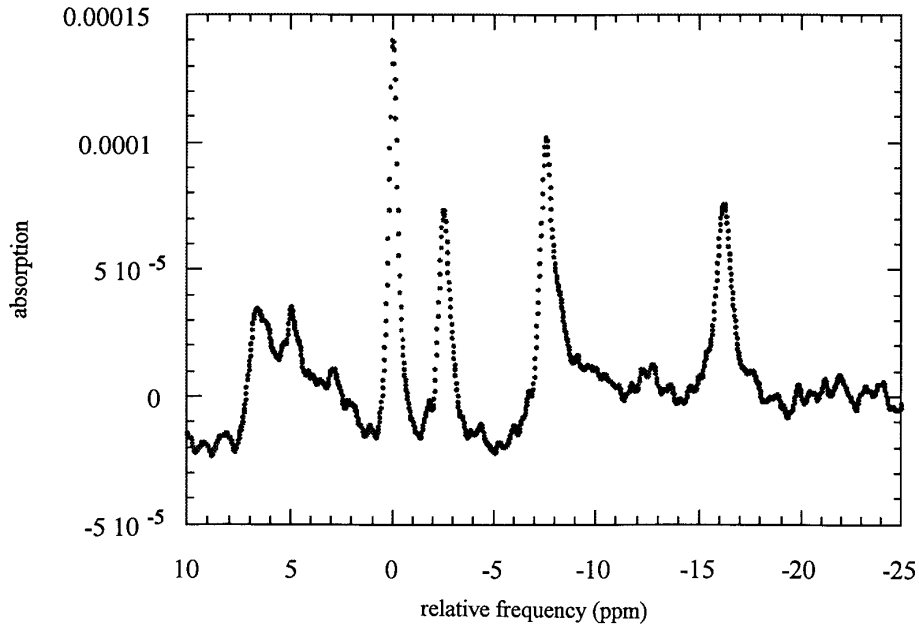

FIG. 1. A typical ^{31}P MRS spectrum obtained from a rat brain *in vivo*. From high to low frequency (left to right) we observe phosphomonoesters, inorganic phosphate (P_i), phosphodiesters, phosphocreatine (PCr) and the three phosphates of ATP (γ-, α-, β-ATP). The frequency (in ppm) is relative to the PCr peak.

at least five times smaller than their experimental results obtained from FT ICR and FT NMR spectra.

We shall be extending this approach to address the effect of complex correlated noise patterns on the errors in determining peak parameters and the mean values associated with a large number of measurements from different spectra where the signal is identical in each spectrum but has a different noise pattern. We shall also show how to determine the appropriate form of the errors in terms of the maximum noise height and the SNR from knowledge of the mean standard deviation and the correlation length of the noise. Conventionally, the SNR is defined as the height of the signal/σ, where σ^2 is proportional to the sum of the squares of the residuals—for more detail see Ref. (*6*). We shall find it more useful, however, from a practical point of view, to define the SNR very simply as the ratio of the signal height/maximum noise height.

The current study is an extension of our previous work (*2*) and includes a critical examination of the noise-induced errors associated with complex correlated noise patterns in spectra. This will be undertaken by (i) introducing the concepts of statistical theory; (ii) analyzing simulated spectra of different noise patterns; (iii) deriving relatively simple equations for determining the standard deviations required; (iv) comparing the mean values of the determined peak parameters, their standard deviations, and correlation matrix elements obtained from the spectra; and (v) plotting the relationship between different *m* values. In so doing, we hope to provide a deeper insight into the significance of noise-induced errors in estimating free [Mg^{2+}], pH, and phosphorus metabolites from *in vivo* ^{31}P MRS spectra.

IN VIVO MRS SPECTRA

A typical *in vivo* rat brain ^{31}P MRS spectrum is shown in Fig. 1, where the phosphocreatine (PCr), γ-, α-, and β-ATP peaks (in decreasing frequency) are distinct, yet superimposed upon a complex noise spectrum. All spectra were subjected to a zero phase correction on the PCr peak and a first order phase correction on the α-ATP peak and were multiplied with an exponential function corresponding to a 25 Hz line broadening. Prior to determining chemical shift assignments, we removed the broadening component attributed to the immobile phospholipids in the bone and membranes by subtracting a 400 Hz broadening (convolution difference) in order to improve the accuracy of resonance amplitude measurements. Figure 2 illustrates two noise patterns, which are portions of ^{31}P MRS spectra some distance from the ^{31}P peak region at a 10-fold increased amplification. These specific noise patterns, most likely arising from post-acquisition line broadening, are observed in a peak free region of the MRS spectrum and account for the observed fine structure on the signal peaks as shown in some detail in our earlier paper (*2*). Similar ^{31}P MRS spectra are presented by Ingwall (*7*) in Langendorff-perfused rat hearts. The origin of such noise patterns may occur through line broadening to improve signal-to-noise ratios (*8*). In this paper, the origin of the noise is of little concern. In order to tackle the effect of the very characteristic noise in such spectra, we have taken an unconventional approach. We have attempted to quantify a noise spectrum in terms of a mathematical function expressed in terms of frequency and time using the observed noise portion of the spectrum being investigated.

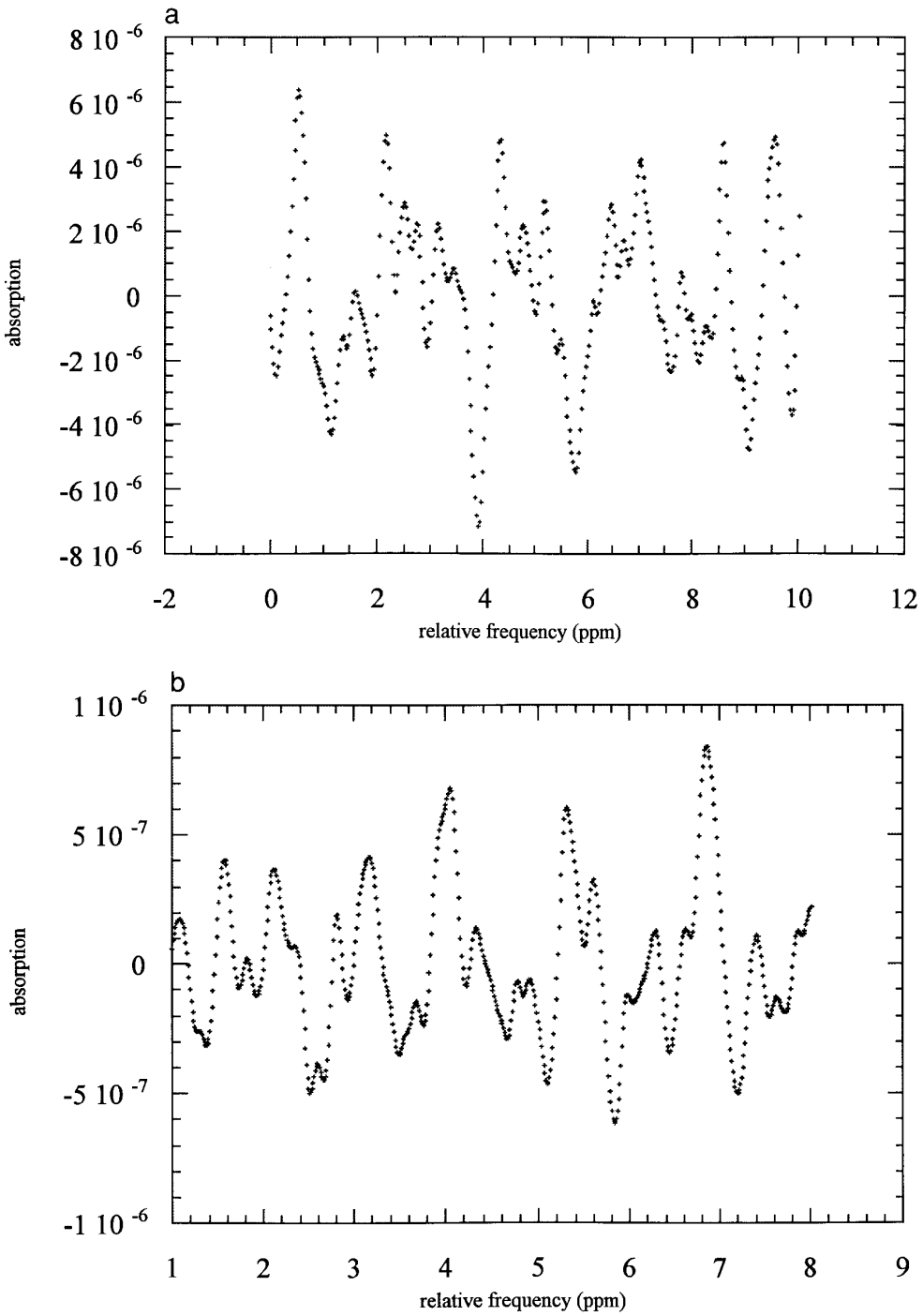

FIG. 2. Two examples of the noise in the ^{31}P MRS spectra obtained from a rat brain *in vivo.* The intensity is 10-fold greater than that in Fig. 1. The frequency (in ppm) is relative to the beginning of the noise spectrum under investigation.

As we will demonstrate, our work may be related to the more conventional approach (*6*). The evidence is that many *in vivo* ^{31}P MRS spectra contain complex correlated noise patterns and it is from such spectra that information about specific ^{31}P nuclei is estimated.

Nevertheless, noise would have arisen from thermal white noise mainly from the coil and the connection to the preamplifier. In addition, the signals plus the white noise are then processed electronically, involving amplification, filters, and Fourier transformation (*6, 9*) to ultimately produce the *in vivo* spectra we consider as our starting point, with its complex noise background. A standard deviation and cor-

relation length characterize the noise from such spectra. We shall show, using this information, how we may define the noise in terms of a frequency and time dependent function involving several random variables. It is this complex function which enables us to gain an insight into the likely errors of any experimentally measured parameters. This background noise we shall refer to as correlated noise in this paper. However, we wish to emphasize that whatever the detailed processes involved in obtaining these spectra, we are dealing with specific spectra which unequivocally comprise NMR signals superimposed upon a complex background of non-signal peaks. The paper uses the experimental observations to examine both the signal and non-signal components. What emerges from this work is that knowledge of the detailed structure of the non-signal component is unimportant in estimating the signal characteristics from the parameters obtained by curve fitting a non-linear equation to a specific peak.

We may confirm the noise pattern in our spectra by examining a portion of a spectrum where no signal peaks are present (see Figs. 2a and 2b). As can be seen we have a series of peaks randomly located across the spectrum. The noise may be described as noise peaks that characterize the frequency dependence of the noise. The example in Fig. 2a comprises approximately 20 noise peaks where the zero phase tends to dominate. In general, however, the phase of the noise randomly varies across the spectrum, as illustrated in Fig. 2b. The selected portion of the noise spectrum of approximately 10 ppm in Fig. 2a may be fitted to 19 Lorentzian or Gaussian lineshapes of constant peak width (about 0.22 ppm) with varying heights and positions but zero phase. It was found that the Lorentzian lineshape, as expected, gives a better fit. The maximum separation of the noise peaks is less than approximately 1 ppm. It is these noise peaks which will limit the signal information we may obtain from our NMR spectra. This may be illustrated further from our earlier paper, where we showed the marked similarity between the observed NMR spectra and the simulated NMR spectra generated by a known signal superimposed upon a series of Lorentzian peaks. Not only were we able to replicate the spectral detail across 20 ppm, but the shape variability of a specific peak was clearly confirmed.

Next we need to consider how best to extract, from a particular NMR peak, information about the signal embedded within the peak. It is important to appreciate the fact that a specific peak comprises both noise and signal. To begin the process of analyzing a specific peak, we shall curve fit a specific shape to the data making up the peak. This will involve fitting a nonlinear equation. In this paper we shall use matrix algebra to achieve this, thereby yielding a set of parameters and their standard errors. The next step is to use this information to determine the signal characteristics.

This may be illustrated very simply by considering a single noise peak and a single signal peak both characterized by two Lorentzian lineshapes given by

$$f_\alpha = \frac{m_1}{(m_2(x_\alpha - m_3)^2 + 1)} + m_4. \qquad [2]$$

We shall choose, for the noise peak, npm_1 = 3, npm_2 = 80 ppm^{-2}, npm_3 = 1.9 ppm, and npm_4 = 0. The units of npm_1 and npm_4 are the same as those of the absorption scale. (The noise peak npm_2 value of 80 ppm^{-2} corresponds to a half-width of about 0.22 ppm, as observed in Fig. 2.) For the signal we shall choose sm_1 = 10, sm_2 = 10 ppm^{-2}, sm_3 = 2.0 ppm, and sm_4 = 0. These two form a single peak; when we analyze it as a single Lorentzian peak (1.4 to 2.6 ppm), we obtain a very good fit that yields the values m_1 = 11.930 (0.169), m_2 = 13.217 ppm^{-2} (0.724 ppm^{-2}), m_3 = 1.973 ppm (0.00209 ppm), and m_4 = 0.257 (0.183). The standard errors are given in brackets. The differences between the curve fitted peak parameters and the signal parameters are far greater than one or two standard errors. It is clear that these standard errors cannot be used to determine the signal parameters from a curve fit of the peak. This paper addresses this problem and shows how to determine the errors in such a way that from a single spectrum we may estimate the signal parameters from the peak parameters obtained from curve fitting. For the above spectrum comprising the two peaks only and knowing that npm_1 = 3 for the noise and sm_1 = 10 for the signal, we shall show that the σ values for this case are given as $\sigma(m_1)$ = 1.287, $\sigma(m_2)$ = 3.03 ppm^{-2}, $\sigma(m_3)$ = 0.0239 ppm, and $\sigma(m_4)$ = 1.056. Similar results will occur using more complex noise backgrounds. Thus we are confident that we can determine the signal characteristics from the peak analysis using our determined σ values. (The "np" and "s" before the m_i values are used to differentiate between the noise (np) and signal (s) peaks. No prefix normally implies that the m_i values are obtained from the peak analysis.)

Another aspect that requires consideration is the form of the equation in determining the peak characteristics. This may be categorized into the shape and a baseline. We shall consider Lorentzian and Gaussian lineshapes. In addition, we need to consider the phase of the signal. In this paper the spectra have been collected in the absorption mode and no attempt has been made to adjust for a dispersion mode component. Inclusion of a small dispersion mode component into the signal would affect the parameters obtained by fitting the signal to only an absorption model. The differences may easily be determined. As an example, if the signal is defined as sm_1, sm_2, sm_3 = 2.000 and sm_4 = 0, replacing m_1, m_2, m_3, and m_4 in Eq. [2], and has a 5% dispersion mode component, then the m_1, m_2, m_3, and m_4 values obtained by fitting a full absorption mode curve fit are, to a very good approximation,

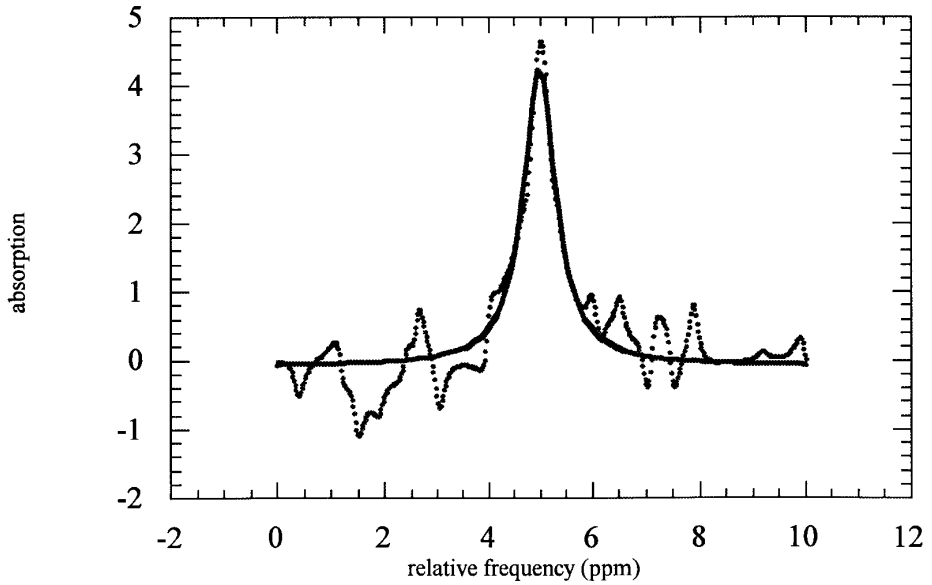

FIG. 3. An example of a simulated spectrum with one signal embedded in a noise spectrum of Lorentzian shaped peaks generated randomly by height and position with random phase. The SNR is defined as 5:1. The curve fitted single Lorentzian lineshape peak is superimposed on the spectrum.

$$m_1 = 1.051\ sm_1$$

$$m_2 = 0.28 + 0.801\ sm_2$$

$$m_3 = 2.085$$

$$m_4 = -0.0510\ sm_1.$$

Varying sm_1 does not affect m_2 and m_3 but sm_2 does slightly affect m_1, m_3, and m_4. (A 5% dispersion mode component most likely would be observed.) In this analysis the spectral range was 2.0 ppm.

These would apply across the spectrum, taking into account, obviously, a different sm_3 value. In the present paper we are concerned only with effects that vary significantly across the spectrum and hence affect each signal in the spectrum to a different degree. In this work we are interested in relative values and differences. Hence we shall not consider a dispersion mode component in analyzing our experimental signal peaks.

Another question that needs to be addressed is how one determines the most appropriate baseline. The answer will depend very much on the specific spectral range that is being analyzed. As our approach focused on analyzing a peak, which contained a single NMR signal, we kept the spectral range rather small, as explained in our earlier paper. We chose 1.2 ppm. We considered three baseline options described by the m_4 and m_5 terms in the equation

$$f_\alpha = \frac{m_1}{(m_2(x_\alpha - m_3)^2 + 1)} + m_4 + m_5 x_\alpha. \qquad [3]$$

We found that the frequency dependent baseline term did not improve the analysis and hence we focused on the two cases when m_4 was zero or nonzero, which resulted in analyses for three or four parameters. In particular, we shall show that m_4 must be included to compensate for phase variations in the noise. Observation of such a frequency dependent term could not be justified from the peaks analyzed in the spectra. In addition, we need to bear in mind that in curve fitting it is important to keep the number of parameters as small as possible.

In our earlier paper we compared several techniques in determining the position of the NMR peaks and showed that the curve fit of a Lorentzian lineshape gave superior results compared with the peak picking and the SISCO line fit methods. This is understandable as the curve fit involving a lineshape uses all the peak data. We used two programs to handle the curve fitting of non-linear equations. The Kaleidagraph commercial software, which uses a specific algorithm, gave the equation parameters, their standard errors, the chi square, and the R values. Our own written program in Mathematica used matrix algebra, with the equations given in this paper, and produced the same information plus the correlation matrix elements.

SIMULATION OF MRS SPECTRA

We may simulate a typical *in vivo* MRS spectrum with a single peak superimposed on a multinoise spectrum. The noise spectrum is chosen as a series of randomly determined noise peaks. Such a spectrum is shown in Fig. 3. The peak is a composite of the noise and the signal. An analysis of the peak

is carried out assuming a specific shape of the peak, and a set of parameters with their estimated errors describing the peak is evaluated. We shall define the set of parameters as a set of m_i values and their errors (standard deviations) by σ_i values. The m_i values and the σ_i values are very dependent on the signal and the noise making up the spectrum across the observed peak. Often we are more interested in using the m_i values from the peak analysis to estimate the m_i values for the signal. This may be achieved by determining the average of the peak m_i values with the corresponding standard deviations, $\sigma(m_i)$ values. These values are dependent on the signal and the average noise across the complete spectrum, which we define as χ^2_{noise}. We reiterate that the m_i values and the σ_i values are for a specific peak whereas the mean of a large number of m_i values and the corresponding $\sigma(m_i)$ values may be used to characterize the signal under investigation.

As an illustration, for the simulated spectrum shown in Fig. 3 we have the result from fitting Eq. [3], with $m_5 = 0$, to the signal peak ($sm_1 = 5$; $sm_2 = 10$ ppm^{-2}; $sm_3 = 5$ ppm; $sm_4 = 0$), using a precise analysis for a nonlinear equation, $m_1 = 4.337$; $\sigma_1 = 0.092$; $m_2 = 6.849$ ppm^{-2}; $\sigma_2 = 0.469$ ppm^{-2}; $m_3 = 4.983$ ppm; $\sigma_3 = 0.0081$ ppm; $m_4 = -0.0897$; $\sigma_4 = 0.021$. From 1000 such simulated spectra with the same signal we find that $\sigma(m_1) = 0.365$, $\sigma(m_2) = 2.36$ ppm^{-2}, $\sigma(m_3) = 0.0238$ ppm, and $\sigma(m_4) = 0.0971$ whereas the mean σ values ($\overline{\sigma_i}$ values) are $\overline{\sigma_1} = 0.0877$, $\overline{\sigma_2} = 0.571$ ppm^{-2}, $\overline{\sigma_3} = 0.00556$ ppm, and $\overline{\sigma_4} = 0.0169$. It is the marked differences between $\sigma(m_i)$ and $\overline{\sigma_i}$, which for uncorrelated noise are the same, that are a characteristic of correlated noise. In essence, this paper explores the differences and shows how to predict the eight sigmas, the σ_i values and the $\sigma(m_i)$ values, from specific characteristics of the background noise.

In this paper we show how to calculate: (i) the m_i values and the corresponding σ_i values for a single peak; (ii) the signal m_i values and the corresponding $\sigma(m_i)$ values; and (iii) the χ^2_{noise} value and the correlation length, which lead to a convenient way to estimate the $\sigma(m_i)$ values as functions of the noise height and the SNR. The $\sigma(m_i)$ values are, thus, characteristic of randomly multipeak correlated noise spectrum.

In this paper, spectra were simulated with a Power Macintosh computer using Excel (Microsoft version 5.0), Kaleidagraph (Abelbeck version 3.0.4) and Mathematica (Wolfram Research version 2.2.2.1 and 3.0) software. Results were confirmed with at least two independently written programs. All spectra and graphs presented in this paper were obtained using Kaleidagraph.

CONCEPTS OF STATISTICAL THEORY

We begin with a set of Q observations which may be expressed as $\{f_\alpha, x_\alpha\}$. In the case of an MRS spectrum comprising a signal (or signals) and a series of noise peaks, f_α is the total height at frequency x_α. In order to analyze a specific peak in the spectrum, the peak may be expressed as a mathematical function with n parameters m_i. In other words, the peak is defined as

$$f_\alpha = f\{x_\alpha, m_1, m_2, \ldots, m_n\}. \quad [4]$$

Determination of the n parameters from the Q observations requires the solution of a set of non-linear equations. The equations may be solved by expanding the function in a Taylor series, thereby reducing the problem to one of a linear form where

$$\Delta f_\alpha = f_\alpha^{\text{obs}} - f_\alpha^{\text{calc}} = \sum_{i=1}^{n} \frac{\partial f_\alpha}{\partial m_i} \Delta m_i. \quad [5]$$

We can choose an initial set of the n m-values and determine the Δf_α values to give a $1 \times Q$ **F** matrix. The $n \times Q$ matrix (denoted as matrix **A**) is then determined, where the **A** matrix elements are given by

$$a_{\alpha n} = \frac{\partial f_\alpha}{\partial m_n}. \quad [6]$$

From the **A** and **F** matrices we calculate the $\Delta\mathbf{M}$ matrix, where

$$\Delta\mathbf{M} = (\mathbf{A}'\mathbf{A})^{-1}\mathbf{A}'\mathbf{F}. \quad [7]$$

$\Delta\mathbf{M}$ is the matrix containing the calculated change in m values as elements. The new set of m values is chosen using

$$\mathbf{M}_{\text{new}} = \mathbf{M}_{\text{old}} + q\Delta\mathbf{M}, \quad [8]$$

where q is chosen to aid convergence and $0 \leq q \leq 1$. At convergence it can be shown that the value of $\mathbf{F}'\mathbf{F}$, i.e., $\Sigma_\alpha (f_\alpha^{\text{obs}} - f_\alpha^{\text{calc}})^2$, is a minimum. The $\mathbf{F}'\mathbf{F}$ value is defined as the χ^2 value.

The standard deviation of the m values is given by

$$\sigma_i = [(\mathbf{H}^{-1})_{ii}]^{1/2}\sigma, \quad [9]$$

where the **H** matrix is described by

$$\mathbf{H} = \mathbf{A}'\mathbf{A}. \quad [10]$$

The correlation matrix elements, ρ_{ij}, are calculated by

$$\rho_{ij} = \frac{[(\mathbf{H}^{-1})_{ij}]\sigma^2}{\sigma_i\sigma_j}. \quad [11]$$

The details of the derivations of the above equations are provided by Hamilton (*10*). To determine the peak parameters for a large number of simulated spectra we wrote a special

Mathematica program, which could handle some 1500 spectra in about 12 h when the spectral range was about 2 ppm. At larger spectral ranges it took much longer and easily several days of computing time. The program used Eq. [8], where q was chosen as 0.2 or 0.5 with 40 or 25 iterations. An approximate initial set of m values was judiciously chosen to begin the process. The σ values were determined using Eq. [9] where

$$\sigma = \left\{ \frac{\chi^2}{Q - n} \right\}^{1/2}. \qquad [12]$$

Q is the number of data points and n the number of parameters being determined. In this work it is either 4 or 3 depending on whether or not we treated m_4 as a parameter. The σ-value is expressed in the absorption units. When the SNR was small and certainly less than five the iterative process occasionally converged, in handling multi-peak noise spectra, to unrealistic values such as negative m_1 and m_2 values. Our program was written to prevent this from happening.

To test our program we checked the m-parameters and the sigmas against the commercially available Kaleidagraph curve fitting program which uses the Levenberg–Marquardt algorithm (*11*). The rhos were obtained from Eq. [11].

We shall now examine an MRS spectrum which comprises a single Lorentzian peak defined as

$$f_\alpha = \frac{m_1}{(m_2(x_\alpha - m_3)^2 + 1)} + m_4, \qquad [13]$$

or as a single Gaussian peak defined as

$$f_\alpha = m_1 \exp(-\ln(2) m_2 (x_\alpha - m_3)^2) + m_4, \qquad [14]$$

where x_α represents the observed frequency scale (in ppm), m_1 = peak height, m_2 = 4/(linewidth)^2, m_3 = position of the center of the peak (in ppm), and m_4 = baseline. The frequency interval between consecutive data points is usually a constant, Δx. We have defined $u = (x - m_3)\sqrt{m_2}$ (or $u = (x - m_3)\sqrt{(\ln(2) m_2)}$ and hence $\Delta u = \sqrt{m_2}\Delta x$ (or $\Delta u = \sqrt{(\ln(2) m_2)}\Delta x$). We then define a **G** matrix as

$$\mathbf{G}_{ij} = \mathbf{H}_{ij}\Delta u = \mathbf{H}_{ij}\Delta x \sqrt{m_2} \quad (\text{or } \mathbf{H}_{ij}\Delta x \sqrt{(\ln(2) m_2)}), \qquad [15]$$

where

$$\mathbf{G}_{ij} = \sum_\alpha^N \left(\frac{\partial f_\alpha}{\partial m_i} \right)_\alpha \left(\frac{\partial f_\alpha}{\partial m_j} \right)_\alpha \Delta u. \qquad [16]$$

Provided the intervals between the data points are small and equal, Eq. [16] may be written as

$$\mathbf{G}_{ij} = \int_a^b \frac{\partial f}{\partial m_i} \frac{\partial f}{\partial m_j}\, \partial u, \qquad [17]$$

where the spectrum ranges from $u = a$ to $u = b$. If the center of the peak, at m_3, is close to the mid-point of the spectral data being analyzed, the **G** matrix elements may be written, for both Lorentzian and Gaussian cases, as

$$\begin{aligned}
&G_{11} = k_{11}; \quad G_{12} = m_1 k_{12}/m_2; \quad G_{13} = m_1\sqrt{m_2}k_{13}; \quad G_{14} = k_{14};\\
&G_{22} = m_1^2 k_{22}/m_2^2; \quad G_{23} = m_1^2 k_{23}/\sqrt{m_2}; \quad G_{24} = m_1 k_{24}/m_2;\\
&G_{33} = m_1^2 m_2 k_{33}; \quad G_{34} = m_1\sqrt{m_2}k_{34}; \quad G_{44} = k_{44}.
\end{aligned} \qquad [18]$$

We note that $\mathbf{H}_{ij} = \mathbf{G}_{ij}/(\Delta x\sqrt{m_2})$ and $\mathbf{H}_{ij} = \mathbf{G}_{ij}/(\Delta x(\ln[2]m_2)^{0.5})$ when the peak is Lorentzian and Gaussian, respectively. The k-values for both cases are:

Lorentzian:

$$\left.\begin{aligned}
k_{11} &= \arctan[w] + \frac{w}{(1 + w^2)}\\
k_{12} &= -\frac{\arctan[w]}{4} - \frac{w}{4(1 + w^2)} + \frac{w}{2(1 + w^2)^2}\\
k_{13} &= 0\\
k_{14} &= 2\arctan[w]\\
k_{22} &= \frac{\arctan[w]}{8} + \frac{w}{8(1 + w^2)} - \frac{7w}{12(1 + w^2)^2} + \frac{w}{3(1 + w^2)^3}\\
k_{23} &= 0\\
k_{24} &= -\arctan[w] + \frac{w}{(1 + w^2)}\\
k_{33} &= \frac{\arctan[w]}{2} + \frac{w}{2(1 + w^2)} + \frac{w}{3(1 + w^2)^2} - \frac{4w}{3(1 + w^2)^3}\\
k_{34} &= 0\\
k_{44} &= 2w,
\end{aligned}\right\} \qquad [19]$$

where w = (spectral range)$\sqrt{m_2/2}$. The total area under a Lorentzian peak is $m_1\pi/\sqrt{m_2}$ with a linewidth = $2/\sqrt{m_2}$.

Gaussian:

$$\left.\begin{aligned}
k_{11} &= \frac{\sqrt{\pi}}{\sqrt{2}}\,\mathrm{erf}[\sqrt{2}w]\\
k_{12} &= \frac{w}{2}\exp[-2w^2] - \frac{\sqrt{\pi}}{4\sqrt{2}}\,\mathrm{erf}[\sqrt{2}w]\\
k_{13} &= 0\\
k_{14} &= \sqrt{\pi}\,\mathrm{erf}[w]\\
k_{22} &= -\left(\frac{3w}{8} + \frac{w^3}{2}\right)\exp[-2w^2] + \frac{3\sqrt{\pi}}{16\sqrt{2}}\,\mathrm{erf}[\sqrt{2}w]\\
k_{23} &= 0\\
k_{24} &= w\exp[-w^2] - \frac{\sqrt{\pi}}{2}\,\mathrm{erf}[w]\\
k_{33} &= \left(-2w\exp[-2w^2] + \frac{\sqrt{\pi}}{\sqrt{2}}\,\mathrm{erf}[\sqrt{2}w]\right)\ln[2]\\
k_{34} &= 0\\
k_{44} &= 2w,
\end{aligned}\right\} \qquad [20]$$

where, in this case, w = (spectral range)$\sqrt{(\ln(2)m_2)}/2$. The total area under a Gaussian peak is $m_1\sqrt{\pi}/\sqrt{(\ln(2)m_2)}$ with a linewidth of $2/\sqrt{m_2}$. We note that

$$\mathrm{erf}[z] = \frac{2\sqrt{2}}{\sqrt{\pi}}\int_0^z \exp(-x^2)dx.$$

From Eq. [9] we may determine expressions for the four standard deviations in terms of the k values in Eq. [19] for the Lorentzian case and in Eq. [20] for the Gaussian case and these are given below:

$$\left.\begin{aligned}
\sigma_1 &= (\mathrm{fac})^{1/2}\,\frac{g[1]}{X}\,\sigma\\
\sigma_2 &= \frac{m_2}{m_1}\,(\mathrm{fac})^{1/2}\,\frac{g[2]}{X}\,\sigma\\
\sigma_3 &= \frac{1}{m_1\sqrt{m_2}}\,(\mathrm{fac})^{1/2}\,\frac{g[3]}{X}\,\sigma\\
\sigma_4 &= (\mathrm{fac})^{1/2}\,\frac{g[4]}{X}\,\sigma,
\end{aligned}\right\} \qquad [21]$$

where fac $= \Delta x(m_2)^{0.5}$ for the Lorentzian case and fac $= \Delta x(\ln(2)m_2)^{0.5}$ for the Gaussian case.

The correlation matrix elements follow from Eq. [11] and are

$$\left.\begin{aligned}
\rho_{12} &= \frac{m_2\sqrt{m_2}\Delta x\rho[1,2]}{m_1 X\sigma_1\sigma_2}\,\sigma^2\\
\rho_{13} &= \frac{\Delta x\rho[1,3]}{m_1 X\sigma_1\sigma_3}\,\sigma^2\\
\rho_{14} &= \frac{\sqrt{m_2}\Delta x\rho[1,4]}{X\sigma_1\sigma_4}\,\sigma^2\\
\rho_{23} &= \frac{m_2\Delta x\rho[2,3]}{m_1^2 X\sigma_2\sigma_3}\,\sigma^2\\
\rho_{24} &= \frac{m_2\sqrt{m_2}\Delta x\rho[2,4]}{m_1 X\sigma_2\sigma_4}\,\sigma^2\\
\rho_{34} &= \frac{\Delta x\rho[3,4]}{m_1 X\sigma_3\sigma_4}\,\sigma^2,
\end{aligned}\right\} \qquad [22]$$

where

$$\begin{aligned}
g[\alpha] &= \{k_{\beta\beta}k_{\gamma\gamma}k_{\delta\delta}/6 - k_{\beta\beta}k_{\gamma\delta}^2/2\\
&\quad + k_{\beta\gamma}k_{\beta\delta}k_{\gamma\delta}/3\}^{1/2}\\
\rho[\alpha,\beta] &= k_{\alpha\gamma}k_{\beta\gamma}k_{\delta\delta} + k_{\alpha\beta}k_{\gamma\delta}^2/2\\
&\quad - k_{\alpha\beta}k_{\gamma\gamma}k_{\delta\delta}/2 - k_{\alpha\gamma}k_{\beta\delta}k_{\gamma\delta}
\end{aligned}$$

and

$$\begin{aligned}
X = \{&k_{\alpha\beta}^2k_{\gamma\delta}^2/8 - k_{\alpha\alpha}k_{\beta\beta}k_{\gamma\delta}^2/4 + k_{\alpha\alpha}k_{\beta\beta}k_{\gamma\gamma}k_{\delta\delta}/24\\
&+ k_{\alpha\alpha}k_{\beta\gamma}k_{\beta\delta}k_{\gamma\delta}/3 - k_{\alpha\beta}k_{\alpha\gamma}k_{\beta\delta}k_{\gamma\delta}/4\}^{1/2}.
\end{aligned}$$

$\alpha \neq \beta \neq \gamma \neq \delta$ and α, β, γ, and δ all take the values 1 to 4, and $\rho_{11} = \rho_{22} = \rho_{33} = \rho_{44} = 1$. The correlation matrix, ρ, is $\{\rho_{ij}\}$.

In the case of fitting only the three m values m_1, m_2, and m_3 to the peak (m_4 is not a variable) we have

$$\begin{aligned}
X &= \{-k_{\alpha\alpha}k_{\beta\gamma}^2/2 + k_{\alpha\alpha}k_{\beta\beta}k_{\gamma\gamma}/6 + k_{\alpha\beta}k_{\alpha\gamma}k_{\beta\gamma}/3\}^{1/2}\\
g[\alpha] &= \{k_{\beta\beta}k_{\gamma\gamma}/2 - k_{\beta\gamma}^2/2\}^{1/2}\\
\rho[\alpha,\beta] &= k_{\alpha\gamma}k_{\beta\gamma} - k_{\alpha\beta}k_{\gamma\gamma}.
\end{aligned}$$

In previous work by Posener (*4*), the integral values for a Lorentzian lineshape were taken between plus and minus infinity, which give the results

$$\left.\begin{aligned}
\sigma_1 &= (\sqrt{m_2}\Delta x)^{1/2}\,\frac{2\sigma}{\sqrt{\pi}},\\
\sigma_2 &= (\sqrt{m_2}\Delta x)^{1/2}\,\frac{m_2}{m_1}\,\frac{4\sqrt{2}\sigma}{\sqrt{\pi}},\\
\sigma_3 &= (\sqrt{m_2}\Delta x)^{1/2}\,\frac{1}{m_1\sqrt{m_2}}\,\frac{2\sigma}{\sqrt{\pi}},\\
\sigma_4 &= 0,\\
\rho_{12} &= \frac{1}{\sqrt{2}},\\
\rho_{13} &= \rho_{14} = \rho_{23} = \rho_{24} = \rho_{34} = 0.
\end{aligned}\right\} \qquad [23a]$$

The equivalent set when the spectral range is very large and when the signal is Gaussian is

$$\left.\begin{aligned}
\sigma_1 &= (\sqrt{\ln(2)m_2}\Delta x)^{1/2}\left(\frac{3}{\sqrt{2\pi}}\right)^{0.5}\sigma,\\
\sigma_2 &= (\sqrt{\ln(2)m_2}\Delta x)^{1/2}\,\frac{m_2}{m_1}\,4\left(\frac{1}{\sqrt{2\pi}}\right)^{0.5}\sigma,\\
\sigma_3 &= (\sqrt{\ln(2)m_2}\Delta x)^{1/2}\,\frac{1}{m_1\sqrt{m_2}}\left(\frac{\sqrt{2}}{\ln(2)\sqrt{\pi}}\right)^{0.5}\sigma,\\
\sigma_4 &= 0,\\
\rho_{12} &= \frac{1}{\sqrt{3}},\\
\rho_{13} &= \rho_{14} = \rho_{23} = \rho_{24} = \rho_{34} = 0.
\end{aligned}\right\} \qquad [23b]$$

The σ_i values given by Eq. [21] are only applicable for the single peak measurement and are affected by the specific noise pattern near the peak being analyzed. They are a measure of the errors in the specific m_i values in analyzing the *peak.* They tell us nothing about the errors in the m_i values for the *signal.* In order to determine these errors we need to address the overall results using the m data from several spectral analyses. This leads to the mean values and the corresponding standard deviations, $\overline{m_i}$ and $\sigma(m_i)$.

The $\sigma(m_i)$ values may be expressed as functions of N and S, the maximum noise height and the signal height, respectively, by examining the appropriate Δm_i value. From Eq. [7], it follows that $\sigma(m_1)$ and $\sigma(m_4)$ are proportional to N whereas $\sigma(m_2)$ and $\sigma(m_3)$ are proportional to N/S. This follows since Δm_i, the matrix elements of ΔM, can be shown to be proportional to N or N/S. To a good approximation, the form of Δm_i values reflects the form of $\{\Sigma\ (\overline{m_i} - m_i)^2\}^{1/2}$, which is proportional to $\sigma(m_i)$. We shall examine this in more detail later with an example.

An experimentalist is usually interested in the two values $\overline{m_i}$ and $\sigma(m_i)$, where $\sigma(m_i)$ is a measure of the error due to the noise on the specific $\overline{m_i}$ value. These values would be determined by analyzing a large number of spectra. However in specific cases, and certainly from *in vivo* measurements, spectral information is typically determined from a limited number of spectra. If, however, $\sigma(m_i)$ is known or may be estimated from the noise pattern in a spectrum then, from a single NMR measurement, we have at least an estimate of the error in the measurement of the m_i values. Therefore the present paper primarily focuses on determining the $\sigma(m_i)$ values for a range of noise patterns where the measured signal may be either Lorentzian or Gaussian in shape. The approach taken may be adopted for determining the errors in the parameter measurements of any signal embedded in a simple or complex random correlated noise pattern. This occurs in the many fields of spectroscopy.

RESULTS

The results of statistical theory can now be applied to examining the errors in the measurement of m_1, m_2, m_3, and m_4 of any peak in a MRS spectrum. This is accomplished by analyzing a simulated spectrum generated from a specific noise pattern and a defined signal peak. As we mentioned earlier the challenge was to choose an appropriate frequency and time dependent function, which was relatively simple to handle and yet characterize most, if not all, of the observed noise patterns.

To illustrate the process and to gain an insight into the effect that a wide range of noise patterns may have on the spectral measurements, we shall begin with a noise spectrum generated by a series of Lorentzian peaks defined as

$$\text{noise spectrum} = N * R(1) \sum_n \times \left\{ \cos[2\pi\theta]\,\frac{1}{\{\text{np}m_2(\delta_n - \delta)^2 + 1\}} + \sin[2\pi\theta]\,\frac{\text{np}m_2^{1/2}(\delta_n - \delta)}{\{\text{np}m_2(\delta_n - \delta)^2 + 1\}} \right\}. \qquad [24]$$

$R(1)$ is a random number from 0 to 1; θ, the noise phase, may vary from 0 to 1; N is the maximum noise height; $\delta_n = \delta_{n-1}$ + gap $R(1)$; and the gap is the maximum distance between the noise peaks. The $\text{np}m_2 = 80\ \text{ppm}^{-2}$ in Eq. [24] gives a noise peak with a half-width of close to 0.22 ppm, as observed, for the noise peaks, from the experimental spectra. $R(1)$ will have a mean of 0.5 and a standard deviation of $1/(2\sqrt{3})$. $(R(1))^2$ will have a mean of $\frac{1}{3}$ and a standard deviation of $2/(3\sqrt{5})$. Similar results would be achieved with a normal distribution of random numbers, which would have a standard deviation of approximately 0.25. With random phase the noise spectrum will range from $-N$ to N with a zero mean value. The range and the mean value are, of course, phase dependent. For zero

phase, for instance, the range is from 0 to N with a mean value of 0.5.

The noise spectrum spectral range, np(range), was chosen as being greater than the peak spectral range analyzed. In the simulated cases of multi-peak noise the np(range) was larger than the range below which the results were affected. In other words, by increasing the noise range from the spectral range chosen, a point was reached where a further increase of the noise range did not affect the results of the peak analysis. In the case of one or three noise peaks the approach was different, as will be explained later.

A very important property of this type of analysis is that if N and S are increased by the same factor and the other parameters (including the randomness of the noise spectrum) remain unchanged, the analysis would yield an exact increase in m_1, m_4, σ_1, σ_4, and σ by the same factor, χ^2 would increase by the factor squared, whereas m_2, m_3, σ_2, and σ_3 would remain exactly the same.

Also, if we introduce a frequency scale parameter so that we may change the relative frequency which includes changing $\mathrm{np}m_2$ by $\mathrm{np}m_2/(\mathrm{scale})^2$, $\mathrm{s}m_2$ by $\mathrm{s}m_2/(\mathrm{scale})^2$, $\mathrm{s}m_3$ by $\mathrm{s}m_3 * (\mathrm{scale})$ and Δx by $\Delta x * (\mathrm{scale})$, then the effect of changing the gap in Eq. [24] by a factor and the scale by the same factor only changes the m_2 and σ_2 values by $1/(\mathrm{factor})^2$ and the m_3 and σ_3 values by the factor. The other values, namely, m_1 and σ_1 values, m_4 and σ_4 values, and χ^2 and σ values, remain exactly the same. We shall often utilize these properties in the paper.

Next we direct our attention to the noise and its relationship to χ^2. If the noise did not affect the signal in the analysis then the expression $\Sigma_\alpha\,(f_\alpha^{\mathrm{obs}} - f_\alpha^{\mathrm{calc}})^2$ would become

$$\chi^2_{\mathrm{noise}} = \sum_\alpha\,(f_\alpha^{\mathrm{noise}})^2 = \{\text{noise spectrum}\}^2. \qquad [25]$$

The "noise spectrum" in Eq. [25], in general, is given by Eq. [24]. However, χ^2_{noise} varies across the spectrum due to the random nature of the noise. For a single noise peak,

$$\chi^2_{\mathrm{noise}} = \frac{N^2\pi}{2\sqrt{\mathrm{np}m_2}\Delta x}. \qquad [26]$$

For reasons which will become apparent later, we shall consider, also, χ^2_{noise} for the multi-noise peak spectrum when the phase for the noise is constant across a spectrum, as well as when the phase varies randomly. When the phase is constant across a spectrum the average value of χ^2_{noise} (per ppm^{-1}) may be written as a series, namely,

$$\chi^2_{\mathrm{noise}} = \frac{N^2\pi}{\Delta x\sqrt{\mathrm{np}m_2}}\left\{\frac{1}{3} + \int_0^1 \frac{2}{(4 + \mathrm{np}m_2a^2)}\,da + \int_0^1\int_0^1 \times \frac{2}{(4 + \mathrm{np}m_2(a+b)^2)}\,dadb + \ldots\right\}, \qquad [27]$$

where the nth integral involving the gaps a, b, c, etc., may be written as

$$\sum_{p=0}^{n} (-1)^p \frac{n!}{p!(n-p)!}\, g_n\Big[\overbrace{0,\ldots,0}^{p}\ \overbrace{1,\ldots,1}^{(n-p)}\Big], \qquad [28]$$

where

$$g_n[a, b, c, \ldots, r, s, t] = \frac{1}{m^{n/2}} \times \left\{\begin{array}{l}(K_n^{(0)} + K_n^{(1)}z + K_n^{(2)}z^2 + \ldots + K_n^{(n-1)}z^{n-1})\arctan[z/2] \\ \quad + (L_n^{(0)} + L_n^{(1)}z + L_n^{(2)}z^2 + \ldots + L_n^{(n-2)}z^{n-2})\log[4 + z^2]\end{array}\right\},$$

and where $z = (a + b + c + \ldots + r + s + t)\sqrt{m_2}$. The expression

$$g_n\Big[\overbrace{0,\ldots,0,}^{p}\ \overbrace{1,\ldots,1}^{(n-p)}\Big]$$

in Eq. [28] means that within $a, b, c, \ldots, r, s, t$ which have the integral limits of 0 and 1, we have p of them equal to 0 (it does not matter which ones) whereas $n - p$ values are equal to 1. Recursion formulas for the K and L values are

$$Q_n^{(0)} = -\frac{4}{(n-1)(n-2)}\,Q_{n-2}^{(0)}$$
$$Q_n^{(m)} = \frac{Q_{n-1}^{(m-1)}}{m}. \qquad [29]$$

$Q_n^{(0)} = K_n^{(0)}$ when $n = 1, 3, 5, 7, \ldots$; $Q_n^{(0)} = L_n^{(0)}$ when $n = 2, 4, 6, 8, \ldots$; and $K_1^{(0)} = -L_2^{(0)} = 1$.

The χ^2_{noise} (per ppm) for any gap value may be determined from Eq. [27] by replacing $\mathrm{np}m_2$ by $\mathrm{np}m_2\,(\mathrm{gap})^2$. Below we give nine examples using 12 terms in Eq. [27] where $\mathrm{np}m_2 = 80\ \mathrm{ppm}^{-2}$ and $N = 1$.

if gap = 0.500 ppm then χ^2_{noise} (per ppm) = 30.17

if gap = 0.625 ppm then χ^2_{noise} (per ppm) = 20.86

if gap = 0.750 ppm then χ^2_{noise} (per ppm) = 15.59

if gap = 0.875 ppm then χ^2_{noise} (per ppm) = 12.28

if gap = 1.000 ppm then χ^2_{noise} (per ppm) = 10.05

if gap = 1.125 ppm then χ^2_{noise} (per ppm) = 8.46

if gap = 1.250 ppm then χ^2_{noise} (per ppm) = 7.28

if gap = 1.375 ppm then χ^2_{noise} (per ppm) = 6.38

if gap = 1.500 ppm then χ^2_{noise} (per ppm) = 5.66.

The same results would have been obtained from Eq. [27] by replacing 1 in the integrals, Eq. [28], by the gap value and dividing χ^2_{noise} (ppm^{-1}) by the gap value.

When the phase varies randomly the result for χ^2_{noise} (ppm^{-1}) greatly simplifies to

$$\chi^2_{\text{noise}}\ (\text{ppm}^{-1}) = \frac{N^2\pi}{3\Delta x\ \text{gap}\sqrt{\text{np}m_2}}. \qquad [30a]$$

The companion equation, which measures the correlation, may be expressed as

$$\chi_{\text{noise}}(\nu)\chi_{\text{noise}}(\nu + \delta\nu) = \frac{\chi^2_{\text{noise}}}{(1 + (\text{np}m_2/4)\delta\nu^2)}. \qquad [30b]$$

From Eq. [30b], a plot of $\chi_{\text{noise}}(\nu)\chi_{\text{noise}}(\nu + \delta\nu)$ against $\delta\nu$ will yield χ^2_{noise} and npm_2. Using Eq. [30a], with knowledge of those two values, would yield the gap value. Care, however, needs to be exercised in using Eq. [30b] if the spectral range is not very large. From 1500 simulations of a 10 ppm noise spectrum generated, after a small correction for a finite spectral range, with npm_2 = 80 ppm^{-2} and gap = 0.5 yielded χ^2_{noise} = 116.27 ppm (0.17 ppm) and npm_2 = 80.75 ppm^{-2} (0.38 ppm^{-2}) when $\delta\nu$ ranged from 0 to 1 ppm in steps of 0.1 ppm. (The errors are given in brackets.) From Eq. [30a], χ^2_{noise} = 117.1 ppm. Ideally the number of simulations should be much larger to obtain better agreement.

In addition, we have the relationship:

$$\text{gap} = \frac{2}{\text{peaks}\ (\text{ppm}^{-1})}. \qquad [31]$$

Peaks (ppm^{-1}) is the average number of random peaks per ppm. Experimentally, χ^2_{noise} (ppm^{-1}) and the gap value may be determined readily. (Often Eq. [31] can be used quickly, to a good approximation, if appropriate portions of the noise spectrum are observed, such as in our Fig. 2a.) From these two values the value of npm_2 follows. For example, with N = 1, if χ^2_{noise} (ppm^{-1}) = 5.85 and the gap = 1 then from Eq. [30], npm_2 = 80.1 ppm^{-2}, if χ^2_{noise} (ppm^{-1}) = 5.85 and the gap = 0.625 then from Eq. [30], npm_2 = 205 ppm^{-2} and, if χ^2_{noise} (ppm^{-1}) = 9.36 and the gap = 0.625 then from Eq. [30], npm_2 = 80.1 ppm^{-2}. It is the χ^2_{noise} (ppm^{-1}), or the noise σ_{noise} value, and the gap, or the correlation length, which characterizes the noise spectrum. Equations [30a], [30b], and [31] enable us to calculate, from the noise spectrum, the noise standard deviation, σ_{noise}, from χ^2_{noise}, the gap value or the correlation length, and then the npm_2 value, thus describing the Lorentzian lineshape, which we have defined as characterizing the correlated noise.

We may determine, from Eq. [30], when the correlated noise approximates the uncorrelated case. The gap may be replaced by Δx and we would expect the linewidth of the correlated noise to be less than Δx. Thus χ^2_{noise} (ppm^{-1}) would be less than $N^2\pi/(6\Delta x)$ or less than $26.2N^2$; i.e., for the uncorrelated noise the σ_{noise} value would be less than $N\sqrt{(\pi/6)} = 0.72N$, and this value is about 1.25 times larger than the uncorrelated σ_{noise}-value of $N/\sqrt{3}$, with a noise range of $-N$ to N.

We may check our simulated noise spectra by determining the χ^2_{noise} (ppm^{-1}) and the gap values. Choosing npm_2 = 80 ppm^{-2}, Δx = 0.02 ppm, and gap = 1, we obtain χ^2_{noise} (ppm^{-1}) = 5.85 (N = 1). Choosing a noise range of 5 ppm, and a spectral range of 1.2 ppm then from 6000 simulated spectra, where the noise phase is random, we obtain χ^2_{noise} (ppm^{-1}) = 5.90, with a large standard deviation of 5.01, and a gap value of 0.994 ppm.

It is clear that the phase, although random when examined over a large number of spectra, may be more accurately described by approximating a specific value over a limited spectral range in a specific spectrum. This will be particularly true when the number of noise peaks in the spectrum under investigation is very small, say, less than 10. Hence this effect must be taken into account in determining the form of the equation to be used to characterize the signal. The inclusion of the m_4 term will handle variations of phase within the noise spectrum. We found that, although m_4 was very phase dependent and $\sigma(m_4)$ phase sensitive the other $\sigma(m_i)$ values, to a good approximation, were independent of the phase. In addition, the form of the $\sigma(m_i)$ values as functions of N and S, as predicted, is only achieved using the m_4 value in curve fitting the signal. We have shown that if the problem were reduced to only three parameters then the $\sigma(m_2)$ and $\sigma(m_3)$ values from simulated spectra, for example, would not be proportional to N/S as expected.

With this as background, we shall now use some examples to illustrate how we can calculate the associated errors.

The Effect of a Single Noise Peak

We shall choose the noise peak as Lorentzian (see Eq. [24], where N = 0.25, 0.5, 0.75, and 1 with $R(1)$ set at unity) and allow the noise peak to move from 0.5 to 3.5 ppm at 0.01 ppm intervals (i.e., np(range) = 3.0 ppm). The phase of the noise is chosen as zero. The results we are determining are independent of the noise phase to a very good approximation and this will be discussed later. Note that the same results would be obtained by allowing the noise peak to randomly move between 0.5 and 3.5 ppm. The signal (Lorentzian lineshape) is defined by Eq. [2], where the signal m_1 value varies from 5 to 20 with signal m_2 = 10 ppm^{-2}, signal m_3 = 2 ppm, and signal m_4 = 0. Later we shall vary the signal m_2 value. The spectral range (i.e., ns(range)) was chosen as 1.2 ppm with intervals (Δx) of 0.02 ppm. The peak is analyzed using Eq. [8] and the peak values m_1, m_2, m_3, and m_4 are determined. The peak m_i values are markedly dependent on the position of the noise peak, as illustrated in Figs. 4a and 4b for m_1 and m_3. It can be shown that for SNR values greater than 5,

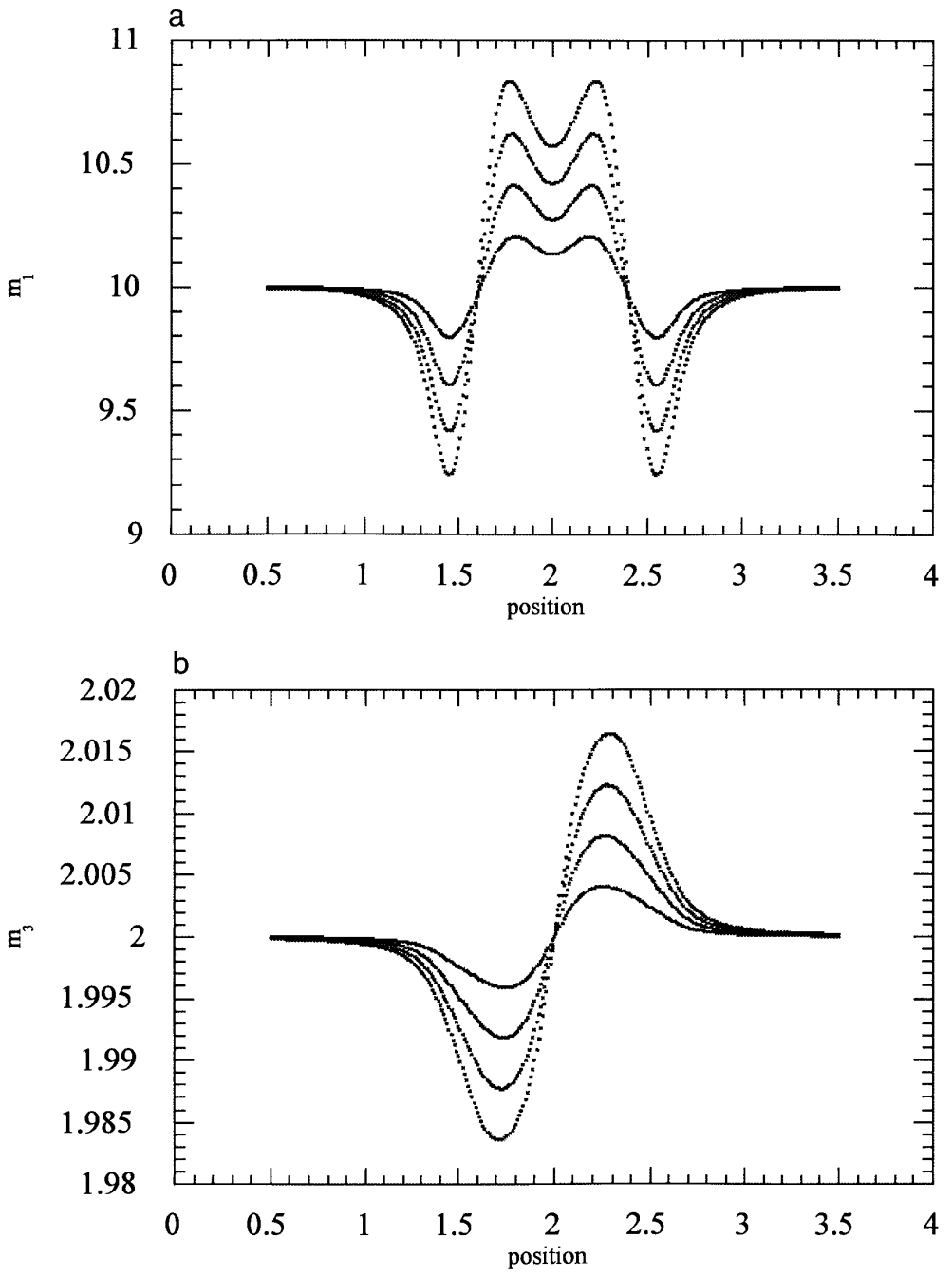

FIG. 4. The m_i value as a function of the position of the single noise peak for four cases when the noise peak height is 0.25 (inner curve), 0.5, 0.75, and 1.0 (outer curve). The Lorentzian signal is at the position 2.0 ppm with a height of 10. (a) $m_i = m_1$. (b) $m_i = m_3$.

$$m_i \propto (N)\, f \quad (\text{for } i = 1 \text{ and } 4)$$
$$m_i \propto (N/S)\, f \quad (\text{for } i = 2 \text{ and } 3),$$

where f is a function of the position of the noise peak and the signal m_2 value. For example, in Fig. 4b,

$$m_3 = 2 + N/S * (\text{position} - 2) * \exp[-6.6 * (\text{position} - 2)^2]. \quad [32]$$

This shows that $\sigma(m_i)$ for SNR values greater than 5 are proportional to N (when $i = 1$ and 4) and proportional to SNR (when $i = 2$ and 3).

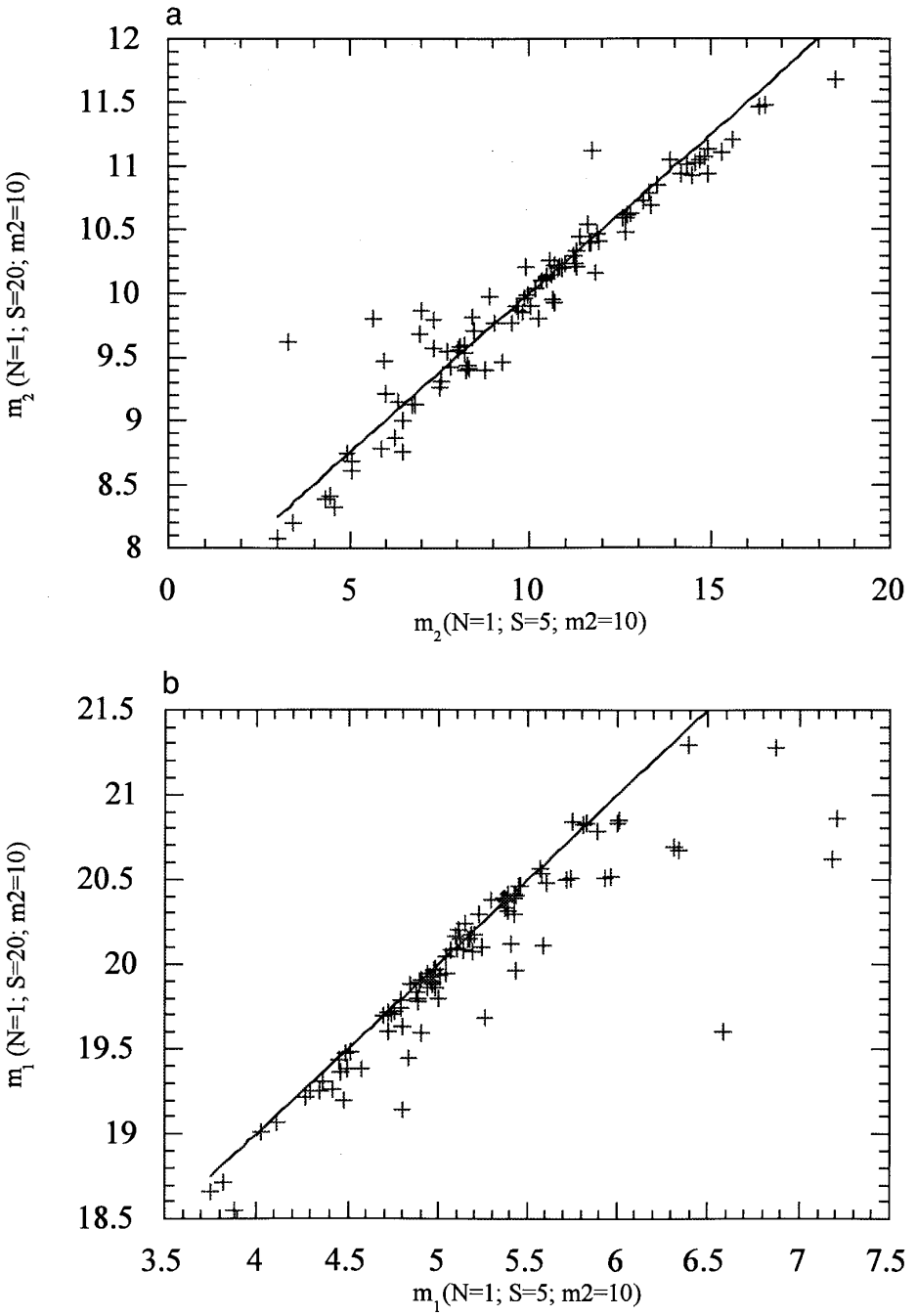

FIG. 5. (a) A plot of 100 pairs of m_2 values for two different signals with the same noise pattern. The line is given by $(m_2\text{-}10)_{y\text{-axis}} = (5/20) * (m_2\text{-}10)_{x\text{-axis}}$. (b) A plot of 100 pairs of m_1 values for two different signals with the same noise pattern. The line is given by $(m_1\text{-}20)_{y\text{-axis}} = (1/1) * (m_1\text{-}5)_{x\text{-axis}}$.

Using the Δm_i values also yields the same N and S dependence and is a general property unrestricted by the complexity of the noise pattern. Figures 5a and 5b provide two examples where the results from 100 multinoise simulated spectra are matched for two different signal parameters. For the peak m_1 value case the slope is 1.0 (the N value is the same) whereas for the peak m_2 case the slope is 0.25 (the ratio of the N/S values is 5/20). In contrast to the signal m_1 value (S) and N, it should be noted that the signal m_2 value does not factor out. Varying the signal m_2 value affects the form of the above function. In Eq. [32], for example, this would correspond to changing the number 6.6 for different signal m_2 values. We obtain the following results, which may be obtained by analyzing the specific data or integrating the appropriate functions such as Eq. [32]:

Signal—Lorentzian

$$\left.\begin{aligned}\sigma(m_1) &= 0.429N\\ \sigma(m_2) &= 10.1(N/S)\\ \sigma(m_3) &= 0.0796(N/S)\\ \sigma(m_4) &= 0.352N.\end{aligned}\right\} \quad [33]$$

Signal—Gaussian

$$\left.\begin{aligned}\sigma(m_1) &= 0.335N\\ \sigma(m_2) &= 6.70(N/S)\\ \sigma(m_3) &= 0.0708(N/S)\\ \sigma(m_4) &= 0.270N.\end{aligned}\right\} \quad [34]$$

The peak was analyzed using a Lorentzian lineshape for the results in Eq. [33] and Gaussian for the results in Eq. [34]. These results, to a very good approximation, are phase independent. For example, from an examination of 20 phase values between 0 and 1 we obtain the following results when $S = 5$ and a Lorentzian lineshape:

$$\left.\begin{aligned}\sigma(m_1) &= 0.442\ (0.011) \quad [\sigma(m_1) = 0.429]\\ \sigma(m_2) &= 2.13\ (0.11) \quad [\sigma(m_2) = 2.02]\\ \sigma(m_3) &= 0.0158\ (0.0019) \quad [\sigma(m_3) = 0.0159]\\ \sigma(m_4) &= 0.0.383\ (0.017) \quad [\sigma(m_4) = 0.0.352].\end{aligned}\right\} \quad [35]$$

The standard deviations are given in curved brackets. On the right, in square brackets, are the values obtained from Eq. [33]. In this paper, these differences were relatively insignificant in our exploration of matching the results from simulated multinoise spectra where the likely errors, due to limitations of the finite number of analyses that could be feasibly handled, were much greater.

If the noise range is varied, we may determine a new set of $\sigma(m_i)$ since $(\sigma(m_i))^2$ is inversely proportional to the noise range. For example, the above results were obtained when the noise range was 3 ppm. To obtain the results when the noise range was 14 ppm we would multiply the above results by $(3/14)^{1/2}$.

We may explore the effect of changing the spectral range from 1.2 ppm chosen above. In this case we shall choose the noise range of 8 ppm. In Table 1 we have provided five different spectral range results using a Lorentzian signal of height (sm_1) 5. Note that multiplying the values when the spectral range is 1.2 by $(8/3)^{0.5}$ yields, to a good approximation, the appropriate values from Eq. [33]. These results show that the $\sigma(m_i)$ values are smaller when the spectral range is increased, with the exception of the $\sigma(m_3)$ value, which remains almost constant. Later we shall show how we may relate these results to any multipeak noise spectrum.

TABLE 1

The Results of Changing the Spectral Range on the Standard Deviations of the Average m_i Values Arising from the Interaction of a Single Noise Peak within ±4 ppm of the Signal ($S = 5$)

Spectral range (ppm)	$\sigma(m_1)$	$\sigma(m_2)$	$\sigma(m_3)$	$\sigma(m_4)$
0.75	0.431	1.41	0.00910	0.401
1.2	0.267	1.20	0.00979	0.219
2	0.203	1.14	0.0104	0.133
4	0.175	1.04	0.0105	0.0689
6	0.170	0.998	0.0105	0.0441

The Effect of Three Noise Peaks

Next we replace the single Lorentzian noise peak with three Lorentzian noise peaks where the peak positions are

$$\begin{aligned}\text{peak } 1 &= p,\\ \text{peak } 2 &= p - R(1)\\ \text{peak } 3 &= p + R(1).\end{aligned}$$

The signal height (sm_1) is 5 and the spectral range is 1.2 ppm. When np (the noise range) varies from 0.5 to 3.5 ppm and the height of the three noise peaks varies randomly from 0 to 1, we obtain the following results from the single signal peak analysis:

Signal–Lorentzian

$$\left.\begin{aligned}\sigma(m_1) &= 0.416\ (0.423)\\ \sigma(m_2) &= 1.94\ (1.99)\\ \sigma(m_3) &= 0.0155\ (0.0157)\\ \sigma(m_4) &= 0.345\ (0.347).\end{aligned}\right\} \quad [36]$$

The signal peak was analyzed using a Lorentzian lineshape for the results in Eq. [36]. From Eq. [27], the χ^2_{noise} value is given by

$$\chi^2_{\text{noise}} = \frac{\pi N^2}{\Delta x\sqrt{m_2}}\left\{\frac{1}{2} + \int_0^1 \frac{2}{(4 + m_2a^2)}\,da + \frac{1}{2}\int_0^1\int_0^1 \frac{2}{(4 + m_2(a+b)^2)}\,dadb\right\}. \quad [37]$$

In this case $\chi^2_{\text{noise}} = 11.8N^2$. This is in contrast to the χ^2_{noise} value for the single noise peak of $8.78N^2$ calculated from Eq. [26].

We may use the following relationship to estimate the $\sigma(m_i)$ values of a three peak noise spectrum from the single noise peak analysis:

$$\sigma(m_i)_l = \sigma(m_i)_k * \left(\frac{\text{np(range)}_k * \chi^2_{\text{noise}}}{\text{np(range)}_l * 8.78} \right)^{1/2}. \quad [38]$$

The np(range) for the three noise peaks is greater than 3 since the central noise peak has a range of 3 ppm and the total range is 5. The effective range, in this case, is approximately 4.15 ppm. Hence we may obtain to a good approximation the $\sigma(m_i)$ values for the three noise peaks interacting with the signal (Eq. [38]) using the $\sigma(m_i)$ value results for a single noise peak (Eq. [33]). We obtain the values given in brackets in Eq. [36].

The Effect of n Noise Peaks

We may extend these results for a single noise peak to any pattern of noise peaks using the calculated χ^2_{noise} value (per ppm). From Eq. [27], using 12 terms the χ^2_{noise} value is $10.05N^2$ (per ppm) for the complex noise pattern of a large number of noise peaks where the gap is chosen as unity. The noise peaks will interact with the signal as some function of the distance from the signal as shown for the single noise peak case in Fig. 4. Hence to use the χ^2_{noise} value (per ppm) for a multipeak noise spectrum we need to replace χ^2_{noise} by (spectral range) $* \chi^2_{\text{noise}}$ (ppm^{-1})/np(range)$_i$ in Eq. [38], where (spectral range)/np(range)$_i$ may be expressed as a factor. Therefore, we may rewrite Eq. [38], in order to compare the multi-peak noise with the single noise peak spectrum, as

$$\sigma(m_i)_l = \sigma(m_i)_k * \left(\frac{\text{np(range)}_k * \text{factor} * \chi^2_{\text{noise}}(\text{ppm}^{-1})}{8.78} \right)^{1/2}. \quad [39]$$

In the case when the phase of the noise is random, Eq. [39] simplifies to the expression

$$\sigma(m_i)_l = \sigma(m_i)_k * \left(\frac{\text{np(range)}_k * 2}{3 \text{ gap}} \right)^{1/2}. \quad [40]$$

From Eqs. [39] and [40], if the phase of the noise is constant across the spectrum under investigation, the factor in Eq. [39] is given as

$$\text{factor} = \frac{\chi^2_{\text{noise}}(\text{ppm}^{-1})_{\text{random phase}}}{\chi^2_{\text{noise}}(\text{ppm}^{-1})_{\text{specific phase}}}. \quad [41]$$

We shall explore the results from Eqs. [39] and [40] by simulating multi-noise spectra and comparing the $\sigma(m_i)$ values. The major problem, however, in accomplishing this goal is that we must carry out a very large number of simulations to gain reliable results and this will depend very much on the speed of the computer used. In the final stages of this paper we have been able to considerably increase the number of simulations within realistic times of less than a day, which has enabled the inclusion of the exploration of a wider range of examples. For instance we have used up to 6000 simulations.

TABLE 2
Comparison of the σ Values in Varying the Gap When $S = 10$

Spectrum	Gap (ppm)	$\sigma(m_1)$	$\sigma(m_2)$ (ppm^{-2})	$\sigma(m_3)$ (ppm)	$\sigma(m_4)$
Calculated	1.5	0.495	1.17	0.00919	0.406
Simulated	1.5	0.501	1.21	0.00913	0.434
Simulated (*)	1.5	0.482	1.19	0.00825	0.416
Calculated	1.0	0.607	1.43	0.0113	0.498
Simulated	1.0	0.614	1.49	0.0109	0.536
Simulated (*)	1.0	0.542	1.42	0.00935	0.483
Simulated (**)	1.0	0.551	1.45	0.00916	0.495
Calculated	0.625	0.767	1.81	0.0142	0.630
Simulated	0.625	0.778	1.90	0.0142	0.692
Simulated (*)	0.625	0.646	1.89	0.0107	0.627
Calculated	0.5	0.858	2.02	0.0159	0.704
Simulated	0.5	0.891	2.14	0.0158	0.781
Simulated (*)	0.5	0.684	1.86	0.0117	0.637

Note. The calculated values were determined from the single noise peak analysis given by Eq. [33] using Eqs. [39] and [40]. The simulated noise spectra were obtained using 6000 multinoise spectra results where the noise phase was random and held constant at zero indicated by (*). In one case the phase was held constant at 0.25, indicated by (**).

We shall begin by comparing the $\sigma(m_i)$ values from the single noise peak analysis (Eq. [33]) with the simulated multi-noise peak spectra where the noise spectrum has a random phase and a zero phase for a range of gap values. The spectral range was 1.2 ppm with a Lorentzian signal where $sm_1(S) = 10$ and $sm_2 = 10$ ppm^{-2}. The noise spectrum was chosen to be ± 2.5 ppm about the signal peak. The results are given in Table 2.

The details presented in Table 2 show that we have very good agreement between the calculated and simulated results, especially when the noise phase is random. When the phase is held constant the $\sigma(m_1)$ and $\sigma(m_4)$ values appear to be smaller, especially at smaller gap values.

We may also explore the effectiveness of our model in predicting the way the $\sigma(m_i)$ values vary with spectral range changes. The details are given in Table 3. Here again the model is very successful in predicting the outcomes especially for the random noise case. As before, if the phase is held constant the $\sigma(m_1)$ and $\sigma(m_4)$ values appear to be smaller.

Tables 2 and 3 show that Eqs. [39] and [40] may be used very effectively to predict the $\sigma(m_i)$ values for multinoise peak spectra from the single noise peak data. Agreement is best when the noise phase is random but for more approximate results we must show that it is applicable, in many cases, to any phase. This is important when the simulation process is limited

TABLE 3
Comparison of the σ Values in Varying the Spectral Range When $S = 10$

Spectrum	Range (ppm)	$\sigma(m_1)$	$\sigma(m_2)$ (ppm^{-2})	$\sigma(m_3)$ (ppm)	$\sigma(m_4)$
Calculated	0.75	0.995	1.63	0.0105	0.926
Simulated	0.75	1.02	1.88	0.0102	0.985
Simulated (*)	0.75	0.939	1.78	0.00919	0.910
Calculated	1.2	0.617	1.39	0.0113	0.506
Simulated	1.2	0.614	1.49	0.0109	0.536
Simulated (*)	1.2	0.542	1.42	0.00935	0.483
Calculated	2.0	0.469	1.32	0.0120	0.308
Simulated	2.0	0.459	1.34	0.0115	0.331
Simulated (*)	2.0	0.352	1.29	0.00927	0.275
Calculated	4.0	0.404	1.20	0.0121	0.159
Simulated	4.0	0.385	1.23	0.0115	0.184
Simulated (*)	4.0	0.301	1.02	0.00934	0.136
Calculated	6.0	0.393	1.15	0.0121	0.102
Simulated	6.0	0.376	1.20	0.0119	0.133
Simulated (*)	6.0	0.297	0.950	0.00944	0.0992

Note. The calculated values were determined from the single noise peak analysis given in Table 1 using Eqs. [39] and [40]. The simulated noise spectra results were obtained using multi-noise spectra where the noise phase was random and held constant at zero indicated by (*). The results for the spectral range 0.75, 1.2, and 2 ppm involved 6000 simulations, the 4 ppm spectral range involved 4000 simulations, and the 6 ppm spectral range involved 2500 simulations.

to smaller numbers and then it is essential to minimize the number of random variables when trying to compare the outcomes from the single and multinoise peak cases.

As a key outcome of our above analysis we may use Eqs. [39] and [40] to calculate from Eqs. [33] and [34] the expected $\sigma(m_i)$ values when the noise is characterized by χ^2_{noise} (ppm^{-1}) = 5.85 (random noise) = 10.05 (constant phase) and the gap = 1 ppm. (The factor in this case is 5.85/10.05 = 0.582.) The results are obtained, in this case, by multiplying by $\sqrt{2}$ to give the $\sigma(m_i)$ values

$$\left.\begin{aligned} \sigma(m_1) &= 0.607 * N \\ \sigma(m_2) &= 14.3 * \frac{N}{S} \\ \sigma(m_3) &= 0.113 * \frac{N}{S} \\ \sigma(m_4) &= 0.498 * N. \end{aligned}\right\} \quad [42]$$

Similar results apply, using the same multiplier, when the signal is Gaussian:

$$\left.\begin{aligned} \sigma(m_1) &= 0.474 * N \\ \sigma(m_2) &= 9.48 * \frac{N}{S} \\ \sigma(m_3) &= 0.100 * \frac{N}{S} \\ \sigma(m_4) &= 0.382 * N \end{aligned}\right\}. \quad [43]$$

To complete the single peak analysis we shall examine the effect of changing the signal m_2-value (sm_2) on the peak m_i σ values, $\sigma(m_i)$. For the case when the signal is Lorentzian and sm_2 is varied from 5 to 20 we find that for $\sigma(m_2)$ we have a linear relationship. For the other σ values the relationship is of the form $a + b/sm_2 + c * sm_2$. When the signal height (sm_1) is 10 ($S = 10$) and the noise is unity ($N = 1$) the results are

$$\left.\begin{aligned} \sigma(m_1) &= 0.0760 + 2.84/sm_2 + 0.0068 * sm_2 \\ \sigma(m_2) &= 0.424 + 0.0601 * sm_2 \\ \sigma(m_3) &= 0.00690 + 0.0203/sm_2 - 0.00011 * sm_2 \\ \sigma(m_4) &= -0.048 + 3.44/sm_2 + 0.0054 * sm_2. \end{aligned}\right\} \quad [44]$$

The Effect of Many Noise Peaks

We have estimated above the expected σ-values for the four parameters of a Lorentzian or a Gaussian signal from a single noise peak. To examine this further, we analyzed 1500 simulated spectra when the noise pattern is randomly generated with a gap of unity for a specific signal level. In this example the phase of the noise is set at zero.

By generating 1500 spectra for specific N and S values, we have shown that for the spectral range of 1.2 ppm and a SNR between 2 and 20.

Fitting the Lorentzian signal to a Lorentzian lineshape.

$$\left.\begin{aligned} \sigma(m_1) &= 0.538N + 34\left(\frac{N^5}{S^4}\right) \\ \sigma(m_2) &= 15.0\left(\frac{N}{S}\right) \\ \sigma(m_3) &= 0.0998\left(\frac{N}{S}\right) \\ \sigma(m_4) &= 0.490N + 40\left(\frac{N^5}{S^4}\right). \end{aligned}\right\} \quad [45]$$

The expressions for $\sigma(m_2)$ and $\sigma(m_3)$ are applicable for SNR values as small as 2 whereas the expressions for $\sigma(m_1)$ and $\sigma(m_4)$ should not be used below SNR = 4. Increasing the noise N-value and the signal S-value by the same factor increases $\sigma(m_1)$ and $\sigma(m_4)$ by the same factor but leaves $\sigma(m_2)$ and $\sigma(m_3)$ unaltered.

Fitting the Gaussian signal to a Gaussian lineshape. If we choose the signal to be a Gaussian lineshape and fit the simulated spectrum also to a Gaussian peak we obtain the relationships

$$\left.\begin{aligned}\sigma(m_1) &= 0.416N + 6.9\left(\frac{N^4}{S^3}\right)\\ \sigma(m_2) &= 10.01\left(\frac{N}{S}\right)\\ \sigma(m_3) &= 0.0847\left(\frac{N}{S}\right)\\ \sigma(m_4) &= 0.391N + 7.6\left(\frac{N^4}{S^3}\right).\end{aligned}\right\}$$

As before, the expressions for $\sigma(m_2)$ and $\sigma(m_3)$ are applicable for SNR values as small as 2 whereas the expressions for $\sigma(m_1)$ and $\sigma(m_4)$ should not be used below SNR = 4. These results agree well with our predicted values when the SNR is greater than 5 (see Eqs. [42] and [43]).

To conclude the comparison with simulated spectra we have been successful in examining the results of 1.2 ppm spectra where a Lorentzian shaped signal is embedded in a random noise with random phase where χ^2_{noise} (ppm^{-1}) = 5.85 and the gap = 1.0. For the signal with sm_2 = 10 ppm^{-2} and $sm_1(S)$ = 5, 7.5, 10, 15, and 20, the following $\sigma(m_i)$ values were determined from 6000 simulations:

$$\left.\begin{aligned}\sigma(m_1) &= 0.596N + 1.58\left(\frac{N^3}{S^2}\right)\\ \sigma(m_2) &= 15.1\left(\frac{N}{S}\right)\\ \sigma(m_3) &= 0.111\left(\frac{N}{S}\right)\\ \sigma(m_4) &= 0.510N + 2.41\left(\frac{N^3}{S^3}\right).\end{aligned}\right\} \qquad [47]$$

(The R value from the analysis of the five data sets used to derive Eq. [47] was greater than 0.99 and in the two cases for the $\sigma(m_2)$ and $\sigma(m_3)$ values it was greater than 0.999 with an error of less than 1% in the constants.) We note the very similar results for the case when the noise phase was set at zero, Eq. [42]. In Eq. [42] the $\sigma(m_1)$ and $\sigma(m_4)$ values are lower. Also, with the greater precision, we observe that the $\sigma(m_1)$ and $\sigma(m_4)$ values are slightly dependent on the N/S ratio when N/S is less than 0.2. They are markedly dependent on N/S when N/S is greater than 0.2.

The relationship between the $\sigma(m_i)$ values from the single peak noise analysis and the multipeak noise results greatly simplifies the effort required to estimate the errors due to random peak noise in complex NMR spectra. Once we have determined the $\sigma(m_i)$ values as outlined above we are then in a position to estimate, to a good approximation, the expected $\sigma(m_i)$ values for any signal in a spectrum just from that spectrum. This may be done by first examining the spectra under investigation to estimate χ^2_{noise} (ppm^{-2}) and the gap (the maximum separation of the noise peaks or from the average number of noise peaks per ppm) and the N value (the maximum noise height). An estimate of the signal height then yields the SNR. By using the appropriate equations the $\sigma(m_i)$ values may be predicted.

[46] To conclude this section we examine the effect of changing the signal m_2 value on the $\sigma(m_2)$ and $\sigma(m_3)$ values. The change is reflected in the results given in Eq. [44] from the single noise peak analysis. Using a multipeak noise spectrum of zero phase yields

$$\left.\begin{aligned}\sigma(m_2) &= (10.39 + 0.50sm_2)(N/S)\\ \sigma(m_3) &= (0.0978 + 0.160/sm_2 - 0.00163sm_2)(N/S).\end{aligned}\right\} \qquad [48]$$

COMPARISON OF THE SIGMAS AND THE RHOS

The next step toward understanding the noise–signal interaction is to explore the variance of the sigmas from spectrum to spectrum with randomly produced simulated noise spectra. The analysis of each spectrum yields different values and our sigma equations above suggest that in terms of the peak, m_1, m_2, and the σ value, we have the relationships

$$\left.\begin{aligned}\sigma_1 &= \text{slope}_1 * \sigma\\ \frac{m_2}{\sigma_2} &= \text{slope}_2 * \frac{m_1}{\sigma}\\ \sigma_3 &= \text{slope}_3 * \frac{\sigma}{m_1}\\ \sigma_4 &= \text{slope}_4 * \sigma,\end{aligned}\right\} \qquad [49]$$

where, in addition, if we use our approximate equations, the slopes may be written as

$$\left.\begin{aligned}\text{slope}_1 &= \left\{(\sqrt{m_2}\Delta x)^{1/2}\,\frac{g[1]}{X}\right\}\\ \text{slope}_2 &= \left\{\frac{X}{(\sqrt{m_2}\Delta x)^{1/2} g[2]}\right\}\\ \text{slope}_3 &= \left\{\left(\frac{\Delta x}{\sqrt{m_2}}\right)^{1/2}\frac{g[3]}{X}\right\}\\ \text{slope}_4 &= \left\{(\sqrt{m_2}\Delta x)^{1/2}\,\frac{g[4]}{X}\right\}.\end{aligned}\right\} \qquad [50]$$

We may test these relationships by analyzing 100 simulated spectra with one signal peak and a series of random noise

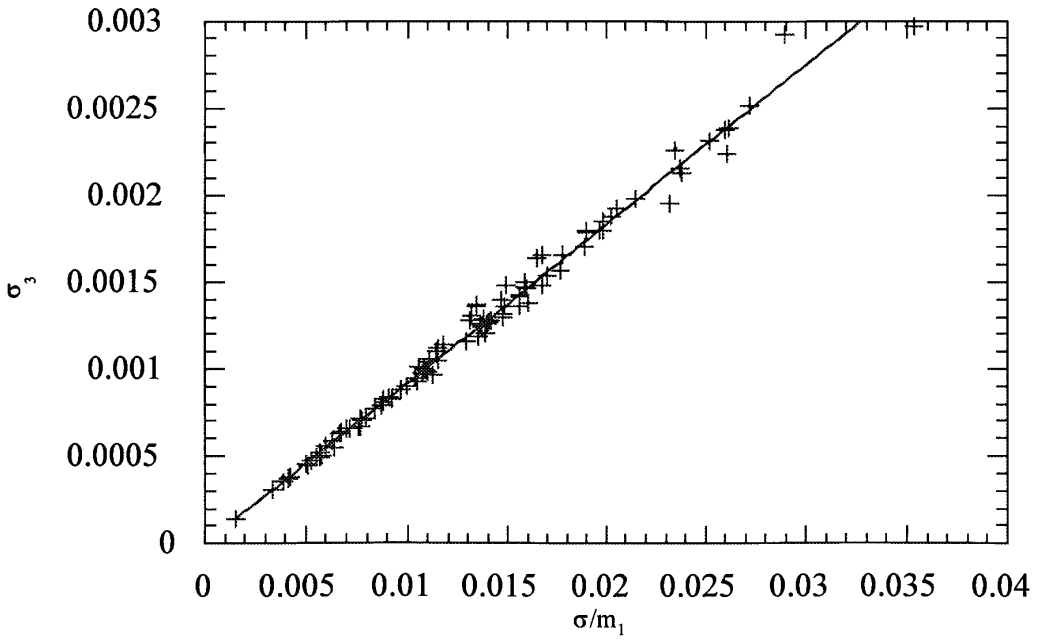

FIG. 6. Plots of the σ_3 value as a function involving σ as expressed in Eq. [49] from the analysis of 100 spectra with one signal peak and a series of random noise peaks.

peaks. The spectral range was chosen as 1.2 ppm and Δx = 0.02 ppm. The Lorentzian shaped signal was defined as sm_1 = 10, sm_2 = 10 ppm^{-2}, sm_3 = 5.0 ppm, and sm_4 = 0. Δx was chosen as 0.02 ppm to closely match the experimental spectra. The four slopes determined by a line of best fit through the origin, with the approximate solutions in brackets, are

$$\left.\begin{aligned} \text{slope}_1 &= 0.731\ (0.740) \\ \text{slope}_2 &= 0.411\ (0.396) \\ \text{slope}_3 &= 0.0917\ (0.0916) \\ \text{slope}_4 &= 0.809\ (0.823). \end{aligned}\right\} \quad [51]$$

Figure 6 shows a typical result. For the 100 spectra, the peak m_1 value varies between 8.99 and 11.12, the peak m_2 between 6.97 and 13.61 ppm^{-2}, the peak m_3 between 4.97 and 5.03 ppm, and the peak m_4 between −0.80 and 1.49. The noise, σ, varies between 0.016 and 0.32. The peak mean values are m_1 = 10.088, m_2 = 10.050 ppm^{-2}, m_3 = 5.0005 ppm, m_4 = 0.299, and σ = 0.133. The mean values of the σ_i-values are σ_1 = 0.0969, σ_2 = 0.328 ppm^{-2}, σ_3 = 0.00122 ppm, and σ_4 = 0.107. We observed that only 20% of the m_3 values lie within the range of 5 ± 2.5 σ_3 of the true signal m_3 value. If we decrease Δx, the σ_i values decrease by the ratio $\sqrt{(\Delta x/0.02)}$ (see Eq. [21]). For example, when Δx = 0.002 the σ_i values are σ_1 = 0.0302, σ_2 = 0.101 ppm^{-2}, σ_3 = 0.000368 ppm, and σ_4 = 0.0335. In this case, less than 10% of pm_3 values lie within 5 ± 2.5 σ_3. A similar effect occurs for the other m_i values.

Next we compare the σ values (σ_i) from each peak analysis and the m_i values and their σ values ($\sigma(m_i)$). The results obtained from the same set of 1500 spectra are given in Tables 4 and 5. The important result is that the $\sigma(m_i)$ values are much greater than the mean σ_i values. The ratios are given in Table 5. This confirmation that the σ_i values should not be used to estimate the errors in the overall m_i values.

We may test the approximate solutions for the σ and ρ values for the single peak analysis. We chose a Lorentzian signal where sm_1 = 5 and a multi-peak noise spectrum, and a series of results is presented in Tables 6 and 7. The set of results in the brackets and braces is calculated from Eqs. [21] and [22], respectively. The additional set for the 10 ppm range is the results given by Eq. [23a]. The multi-peak noise spectrum was the same for each spectrum analyzed. Similar results are obtained for the Gaussian signal case.

The formulas derived for calculating the σ and ρ values for a single peak analysis given by Eqs. [21] and [22] are applicable to a spectral range at least as small as 1.2 ppm. They are

TABLE 4

A Summary of 1500 Peak Sigma Results from 1500 Spectra Comprising a Signal with S = 5 and a Simulated Multi-noise Spectrum Where the Noise Phase Is 0

	σ_1	σ_2 (ppm^{-2})	σ_3 (ppm)	σ_4
Range	1.57	4.69	0.0107	1.63
Mean	0.106	0.634	0.00237	0.116

TABLE 5

A Summary of 1500 Peak m_i Results from 1500 Spectra (1.2 ppm) Comprising a Signal with $S = 5$ and a Simulated Multi-noise Spectrum Where the Noise Phase Is 0

	m_1	m_2 (ppm^{-2})	m_3 (ppm)	m_4
Range	5.90	19.6	0.170	5.97
Mean	5.159	10.137	2.0005	0.222
$\sigma(m_i)$	0.577	2.90	0.0189	0.530
$\sigma(m_i)/\sigma_i$	5.4	4.6	8.0	4.6

a considerable improvement over the formulas suggested by Posener (*4*) and Chen *et al.* (*5*), which are only applicable for very large spectral ranges and are not applicable to *in vivo* NMR analyses where we need to analyze spectra close to a particular peak of interest. The ρ values are of particular interest; for small spectral ranges, ρ_{12} is large and negative. As the spectral range increases it becomes large and positive, tending toward a value of $1/2^{0.5}$. In the Gaussian case it behaves in the same way but tends to a value of $1/3^{0.5}$. On the other hand, ρ_{14} is large and negative for small spectral ranges and approaches zero for large spectral ranges. ρ_{24} is large and positive for small spectral ranges and approaches zero for large spectral ranges. In the Gaussian case ρ_{14} and ρ_{24} behave in the same way. We find the same general pattern for the ρ-values for the m_i values. A typical set of results is shown in Table 8 for three spectral ranges.

Finally, we shall conclude this section by examining the σ values used to determine σ_1, σ_2, σ_3, and σ_4 in Eq. [9]. We may estimate the mean σ value from the mean χ^2 value provided we know the appropriate $\chi^2/\chi^2_{\text{noise}}$ ratio since we can calculate the χ^2_{noise} value from Eq. [27]. The χ^2 value is approximately independent of the noise phase chosen. The $\chi^2/\chi^2_{\text{noise}}$ ratio does vary significantly with the spectral range and is independent of the signal height. From our simulated spectra when the maximum separation of the noise peaks is 1 ppm (gap = 1 ppm) we have the following results, where we have chosen the noise phase as zero:

$$1.2 \text{ ppm spectral range}, \quad k = \chi^2/\chi^2_{\text{noise}} \text{ ratio} = 0.10.$$

$$4.0 \text{ ppm spectral range}, \quad k = \chi^2/\chi^2_{\text{noise}} \text{ ratio} = 0.27.$$

$$10.0 \text{ ppm spectral range}, \quad k = \chi^2/\chi^2_{\text{noise}} \text{ ratio} = 0.34.$$

Hence in our simulated spectra for the 1.2 ppm spectral range the mean σ value is given by $\sigma = \{k\chi^2_{\text{noise}}/(Q - n)\}^{1/2} = 0.145$ absorption units, since $Q = 61$ ($\Delta x = 0.02$) and $n = 4$.

The χ^2 value reflects the degree of the noise "seen" by the analysis as part of the peak. This may be illustrated by a very simple example. If we had a single noise peak with the same width and position as the signal then the analysis would yield $\chi^2 = 0$, because the height of the peak is the sum of the signal and the noise. Although we have a perfect fit the peak height is not the signal height. For this reason we must be very careful in inferring peak information to the signal parameters when handling such noise.

In addition, the χ^2 value and, of course, the χ^2_{noise} value (but not the mean χ^2_{noise} value) vary significantly from spectrum to spectrum. We may explore the smallest likely value from a series of spectra by considering how the χ^2_{noise} value will vary for a specific arrangement of noise peaks. First, the minimum χ^2_{noise} value will occur when the noise peaks are at the maximum separation, i.e., the gap value. If we consider all the peaks to be the same height, h, and equally spaced about the center of the spectrum then

TABLE 6

A Comparison of the σ Values Determined from the Analysis of a Single Spectrum

Range (ppm)	σ_1	σ_2 (ppm^{-2})	σ_3 (ppm)	σ_4
1.2	0.1100 (0.1146)	0.6007 (0.6159)	0.002604 (0.002609)	0.1222 (0.1273)
2	0.07088 (0.07145)	0.6195 (0.6242)	0.004075 (0.004076)	0.06347 (0.06454)
4	0.05763 (0.05765)	0.3767 (0.3774)	0.004122 (0.004122)	0.02653 (0.02668)
10	0.06943 (0.06943)	0.3880 (0.3881)	0.004991 (0.004991)	0.01426 (0.01428)
∞	{0.06938}	{0.3460}	{0.004991}	{0}

Note. The results in brackets and braces were determined from the approximate solutions given by Eqs. [21] and [23a], respectively.

TABLE 7

A Comparison of the ρ Values Determined from the Analysis of a Single Spectrum

Range (ppm)	ρ_{12}	ρ_{13}	ρ_{14}	ρ_{23}	ρ_{24}	ρ_{34}
1.2	−0.797 (−0.808)	0.013 (0)	−0.943 (−0.947)	−0.010 (0)	0.936 (0.938)	−0.013 (0)
2	−0.162 (−0.175)	0.002 (0)	−0.579 (−0.588)	−0.002 (0)	0.833 (0.835)	−0.002 (0)
4	0.388 (0.385)	0 (0)	−0.186 (−0.188)	0 (0)	0.675 (0.676)	0 (0)
10	0.615 (0.614)	0 (0)	−0.035 (−0.035)	0 (0)	0.451 (0.452)	0 (0)
∞	{0.707}	{0}	{0}	{0}	{0}	{0}

Note. The results in brackets and braces were determined from the approximate solutions given by Eqs. [22] and [23b], respectively.

TABLE 8

The ρ-Values for the m_i Values Derived from 4500 (1.2 ppm), 1500 (4.0 ppm), and 500 (10.0 ppm) Simulated Spectra with Multinoise Peaks Where the Signal Was Chosen as Lorentzian with $sm_1 = 5$, $sm_2 = 10$ ppm^{-2}, $sm_3 = 2$ ppm, and $sm_4 = 0$

Range (ppm)	ρ_{12}	ρ_{13}	ρ_{14}	ρ_{23}	ρ_{24}	ρ_{34}
1.2	−0.496	−0.0287	−0.871	0.0353	0.771	0.0346
4.0	0.253	−0.010	−0.118	−0.036	0.623	0.011
10	0.395	−0.013	−0.088	−0.093	0.462	0.029

$$\chi^2_{\text{noise}} = \frac{h^2 2\pi}{\Delta x \sqrt{\text{np}m_2}} \left\{ \frac{1}{4} + \sum_{n=1}^{\infty} \frac{2}{(4 + \text{np}m_2 n^2)} \right\}. \qquad [52]$$

Equation [52] is rather interesting. When $h = 1$ the χ^2_{noise} value (per ppm) given by Eq. [52] is a good approximation of the results from Eq. [27]. (For the case with a random noise phase Eq. [52] simplifies to Eq. [26], where $N = 1$.) (As before, to obtain the χ^2_{noise}-value (per ppm) when the gap is varied $\text{np}m_2 \rightarrow \text{np}m_2 * (\text{gap})^2$.) Table 9 illustrates the similarity of the mean χ^2_{noise} value (per ppm) from Eq. [27] and the χ^2_{noise} value (per ppm) given by Eq. [52] when the gap and the noise peak $\text{np}m_2$ value are varied. In Table 9 the summation in Eq. [52] is over 1000 terms whereas in Eq. [27] we have used only the first 12 terms.

From Eq. [52] we may estimate the χ^2_{noise} value for varying values of the h value which may be the lowest likely value. For example, if we compare some 1500 simulated spectra and wish to estimate the σ-value below which only about 1 in 1500 σ values occurs we may do this by choosing $h = (\frac{1}{1500})^{1/\text{peak}}$, where the peak value is the effective number of peaks corresponding to the particular spectral range. The results are illustrated for three spectral range examples in Table 10. The three observed minimum χ^2 values correspond to the σ values 0.005, 0.0697, and 0.1620. As the spectral range increases the range of the χ^2_{noise}-value decreases and the minimum value will tend to the mean χ^2_{noise}-value. Similar results will apply for any specific or random noise phase.

TABLE 9

A Comparison of the χ^2_{noise} Value (per ppm^{-1}) from Eqs. [27] and [52] for Three Different Noise Peak m_2 Values and Gap Values

Gap (ppm)	$\text{np}m_2 = 80$ ppm^{-2}		$\text{np}m_2 = 10$ ppm^{-2}		$\text{np}m_2 = 200$ ppm^{-2}	
	Eq. [27]	Eq. [52]	Eq. [27]	Eq. [52]	Eq. [27]	Eq. [52]
1.375	6.38	6.93	31.6	29.2	3.49	4.18
1.000	10.05	10.18	54.7	51.2	5.27	5.91
0.625	20.86	19.52	125.3	126.7	10.2	10.3

TABLE 10

Estimation of the χ^2 Value below Which Only about 1 in 1500 χ^2 Values Occur

Spectral range (ppm)	Number of effective peaks	χ^2_{noise} Value	χ^2 Value	Observed minimum χ^2 value
1.2	2	0.0120	0.0012	0.0015
4	6	3.53	0.95	0.956
10	12	29.8	10.1	13.0[a]

[a] The observed minimum χ^2 value when the spectral range was 10 ppm was from only 500 simulated spectra.

The effect of the noise component as reflected above is in marked contrast to the case when the noise contribution of each data point has a normal distribution with a zero mean and a standard deviation equal to σ and the noise contribution of successive data points is uncorrelated. It has been shown that with such a noise background this σ-value dictates a lower bound, known as the Cramér–Rao lower bound (*12*), and is the minimum possible value for the σ value in Eq. [9].

Such a noise background would be less than 10% of our total noise component observed in our *in vivo* spectra. Thus, if such a noise background were superimposed upon our simulated spectra the minimum σ value would be approximately 0.025. From our above analysis we would only observe the Cramér–Rao lower bound when the spectral range is rather small, and in this work it has no real significance.

Finally, in this section we compare our results for a correlated noise example with the case when the noise is uncorrelated. We shall focus on the example when the signal may be described by a Lorentzian function. For the correlated noise case, with random phase, our χ^2_{noise} (ppm^{-1}) $= 5.85N^2$ (or $\sigma_{\text{noise}} = 0.312N$) and the gap = 1.0 ppm ($\sigma_{\text{noise}} = \{\chi^2 \Delta x / (\text{spectral range}\}^{0.5}$. The χ^2_{noise} value standard deviation is about $5.79N^2$, which is very large. For a spectral range of 1.2 ppm the mean χ^2 value is about $1.40N^2$, yielding a σ value of $0.157N$. Using Eq. [21] we may estimate the mean σ_i values as approximately

$$\left.\begin{aligned} \sigma_1 &= 0.116N \\ \sigma_2 &= 3.95 \frac{N}{S} \\ \sigma_3 &= 0.0144 \frac{N}{S} \\ \sigma_4 &= 0.129N. \end{aligned}\right\} \qquad [53]$$

From 6000 simulated spectra we find the following results when $sm_1 = 10$ and $N = 1$, i.e., the noise range is from −1 to 1: $\chi^2 = 1.40$, $\sigma_1 = 0.101$ (0.116), $\sigma_2 = 0.340$ ppm^{-2} (0.395 ppm^{-2}), $\sigma_3 = 0.00126$ ppm (0.144 ppm) and $\sigma_4 = 0.112$

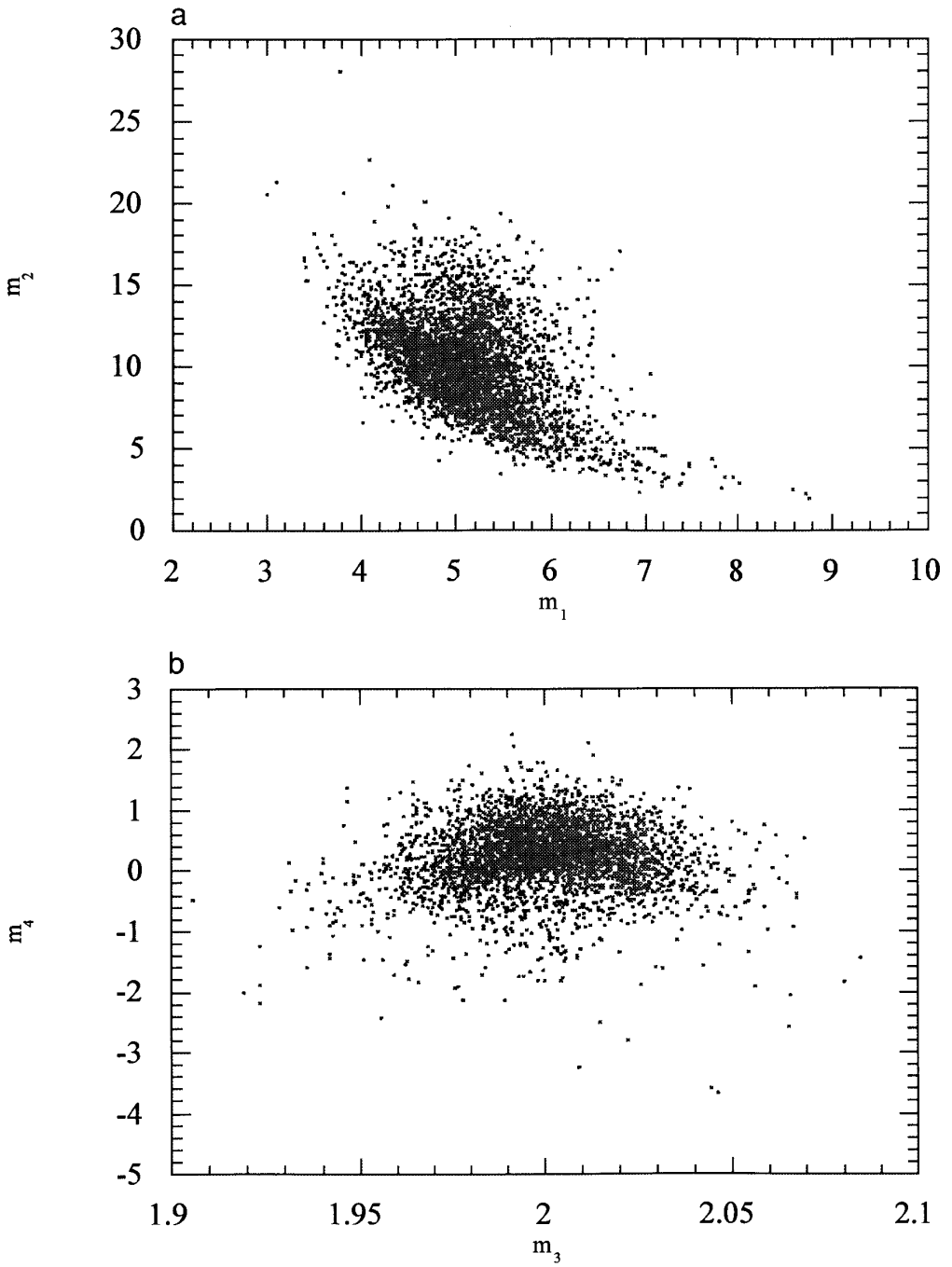

FIG. 7. Plots of the m values from the analysis of the single peak from 4500 simulated spectra where the signal was expressed by Eq. [2] with $sm_1 = 5$, $sm_2 = 10$ ppm^{-2}, $sm_3 = 2.0$ ppm, and $sm_4 = 0$. The spectral range was 1.2 ppm. (a) m_2 versus m_1 and (b) m_4 versus m_3.

(0.129). The results in brackets are from Eq. [53] and considering the approximations involved show remarkable agreement between the calculated and mean sigma observed values.

Next we turn to the case when the noise is uncorrelated. If the noise height randomly varies between $-N$ and N with a uniform distribution then $\chi^2_{\text{noise}} = \{(\text{spectral range})/\Delta x + 1\}(\frac{1}{3}) = 20.33N^2$, $\sigma_{\text{noise}} = 0.582N$. The standard deviation of the χ^2_{noise}-value may be expressed as $\{(\text{spectral range})/\Delta x + 1\}^{0.5}(2/(3\sqrt{5}))$, which is 2.33 when the spectral range is 1.2 and $\Delta x = 0.02$. But in this case, we would expect $\chi^2 = \chi^2_{\text{noise}}$. From 6000 simulations we find that, when the spectral range is 1.2 ppm, $\chi^2 = 19.0N^2$ instead of $20.33N^2$. (This small

reduction is in marked contrast to the very large difference that occurs in the correlated case.) Using this χ^2 value we may estimate the mean σ_i values, and hence the $\sigma(m_i)$ values, from Eq. [21]. (The σ value is given by Eq. [12].) The results are

$$\left.\begin{aligned} \overline{\sigma_1} &= \sigma(m_1) = 0.427N \\ \overline{\sigma_2} &= \sigma(m_2) = 14.6\,\frac{N}{S} \\ \overline{\sigma_3} &= \sigma(m_3) = 0.0529\,\frac{N}{S} \\ \overline{\sigma_4} &= \sigma(m_4) = 0.475N. \end{aligned}\right\} \qquad [54]$$

(As the spectral range increases the numbers in Eq. [54] tend to the following: $0.427 \rightarrow 0.164$, $14.6 \rightarrow 4.63$, $0.0529 \rightarrow 0.0518$, and $0.475 \rightarrow 0$.)

From the 6000 simulations when $sm_1 = 10$ we find $\sigma_1 = \sigma(m_1) = 0.418$ (0.427), $\sigma_2 = \sigma(m_2) = 1.42$ ppm^{-2} (1.46 ppm^{-2}), $\sigma_3 = \sigma(m_3) = 0.00526$ ppm (0.00529 ppm), and $\sigma_4 = \sigma(m_4) = 0.464$ (0.475). The results in brackets are from Eq. [54]. We find very good agreement. If the random height distribution of the uncorrelated noise were a normal distribution, with a standard deviation of σ, then the numbers in Eq. [54] would be multiplied by $\sigma\sqrt{3}$ to give the equivalent mean σ_i values and hence the $\sigma(m_i)$ values. For a normal distribution with a zero mean and $\sigma = 0.50$, about 95% of the noise height lies between -1 and 1. In this case $\sigma\sqrt{3} = 0.866$. An important aspect is that Eq. [47] cannot be obtained from Eq. [54], or Eq. [53], using a single multiplying factor, e.g., $15.1/14.6 = 1.03$, whereas $0.111/0.0529 = 2.14$.

This section has shown that we have been able to derive equations to successfully predict the standard deviations of the peak parameters. These equations are expressed as functions of the maximum (or minimum) noise height (N), where the noise varies randomly from $-N$ to N, and the signal height (S), where the noise may be described as uncorrelated or correlated. The differences between the eight sigmas for the correlated and noncorrelated noise patterns are very significant.

RELATIONSHIP BETWEEN THE MULTI-PEAK AND SINGLE PEAK NOISE ANALYSES

In an earlier section we showed how to derive the standard deviation of each of the four m values arising from a noise spectrum comprising multinoise peaks generated randomly from a single noise spectrum and a three noise spectrum. In this section we shall explore the errors expected in the four m values in a different way. Using a large series of simulated spectra with a single signal superimposed on a multinoise peak spectrum (random peak height and position) we may readily determine the range of the m values. This is illustrated by plotting a couple of different m values obtained from a large number of analyses. Figures 7a and 7b illustrate the spread of the m values obtained from the analysis of 4500 simulated spectra for the case when the spectral range is 1.2 ppm and the Lorentzian signal has the parameters $sm_1 = 5$, $sm_2 = 10$ ppm^{-2}, $sm_3 = 2$ ppm, and $sm_4 = 0$. These m plots form very characteristic patterns and highlight the spread and the frequency of the results. The range of results given in Table 5 is reflected in these plots.

If we use a single noise peak of a specific height, N, and determine the effect of this noise peak on the measurement of the peak parameters we obtain a set of contours for the two m-plots, as shown in Figs. 7a and 7b. These are shown in Figs. 8a and 8b. The corresponding m-plots are very similar and mirror the complex patterns. The majority of the data points are within the contour of $N = 1.5$ and almost all are within the contour of $N = 2.0$. Using the value $N = 1.5$ we obtain

$$\left.\begin{aligned} m_1 &= 5 \pm 1.21 \\ m_2 &= 10 \pm 6.35 \\ m_3 &= 2 \pm 0.0528 \\ m_4 &= 0 \pm 1.24. \end{aligned}\right\} \qquad [55]$$

These results are very close to $m_i \pm 2\sigma(m_i)$. Hence this simple approach may readily yield the expected errors in the m_i-values describing a particular signal obtained from the analysis of a peak, a composite of random noise and the signal. In addition, it reinforces our approach in predicting the appropriate $\sigma(m_i)$ values from the single noise peak analysis.

CHARACTERIZATION OF THE PEAK LINESHAPE

We next examined the analysis of either a Lorentzian or a Gaussian lineshape and then used the two results to gain information about the peak's lineshape. With this in mind, we analyzed a Gaussian and a Lorentzian peak superimposed on the usual random Lorentzian noise spectrum and fitted the result to a Lorentzian and a Gaussian peak. The signal height (sm_1) range was from 2 to 20 with a 1.2 ppm spectral range. For the m_1 values we obtained, using a Lorentzian signal ($R = 0.9996$),

$$m_1\text{-Lorentzian fit} = 1.306 * m_1\text{-Gaussian fit.} \qquad [56]$$

Using a Gaussian signal ($R = 0.9995$), we obtained

$$m_1\text{-Lorentzian fit} = 1.406 * m_1\text{-Gaussian fit.} \qquad [57]$$

Although the errors in the m_2 values are greater, we find a similar relationship. For the case when the signal is Lorentzian ($R = 0.978$),

$$m_2\text{-Lorentzian fit} = -4.1 + 0.98 * m_2\text{-Gaussian fit}, \quad [58]$$

and for the Gaussian case ($R = 0.968$),

$$m_2\text{-Lorentzian fit} = -2.5 + 0.83 * m_2\text{-Gaussian fit}. \quad [59]$$

These results are clearly different and, where appropriate, may be used to determine the best peak shape from the analysis of the experimental data.

ANALYZING *IN VIVO* ^{31}P MRS SPECTRA

We conclude this paper by examining six sets of α- and β-ATP ^{31}P MRS measurements obtained from rat brain *in vivo*, where each set is a series of nine measurements over a 4 h period following moderate fluid percussion-induced brain injury. Each set consists of an average of acquisitions in 30 min blocks obtained over a 4 h period after the injury. The 54 ^{31}P MRS spectra were analyzed with the α- and β-ATP ^{31}P peaks at the center of a small spectral range for a Lorentzian and a Gaussian lineshape. A typical analysis—the β-ATP ^{31}P peak in Fig. 1—yields, for a Lorentzian lineshape, $m_1 = 8.62 \times 10^{-5}$, $\sigma_1 = 2.22 \times 10^{-6}$ (2.45×10^{-6}), $m_2 = 4.22$ ppm^{-2}, $\sigma_2 = 0.246$ ppm^{-2} (0.265 ppm^{-2}), $m_3 = -16.164$ ppm, $\sigma_3 = 0.00178$ ppm (0.00180 ppm), $m_4 = -9.65 \times 10^{-6}$ and $\sigma_4 = 2.37 \times 10^{-6}$ (2.61×10^{-6}). The values in brackets are calculated from Eq. [21], where the spectral range is 1.206 ppm and $\sigma = 1.10 \times 10^{-6}$. The good agreement is in marked contrast to the results of Chen *et al.* (*5*).

We may extend our peak analysis to the α- and β-ATP ^{31}P peaks in a single spectrum where we select two portions each about 1.2 ppm, one with the α-ATP ^{31}P peak near the middle and the other with the β-ATP ^{31}P peak close to the middle of its spectral range. A typical set of results, fitting a Lorentzian lineshape to the two peaks, is given below.

α-ATP ^{31}P peaks	β-ATP ^{31}P peaks
$m_1 = 6.76 \times 10^{-5}$	$m_1 = 10.3 \times 10^{-5}$
$\sigma(m_1) = 1.94 \times 10^{-6}$ (2.22×10^{-6})	$\sigma(m_1) = 2.92 \times 10^{-5}$ (3.92×10^{-5})
$m_2 = 8.126$ ppm^{-2}	$m_2 = 1.04$ ppm^{-2}
$\sigma(m_2) = 0.734$ (0.807) ppm^{-2}	$\sigma(m_2) = 0.400$ (0.521) ppm^{-2}
$m_3 = -7.534$ ppm	$m_3 = -16.051$ ppm
$\sigma(m_3) = 0.00347$ (0.00340) ppm	$\sigma(m_3) = 0.00648$ (0.00600) ppm
$m_4 = 1.91 \times 10^{-4}$	$m_4 = -2.38 \times 10^{-6}$
$\sigma(m_4) = 2.14 \times 10^{-6}$ (2.45×10^{-6})	$\sigma(m_4) = 2.96 \times 10^{-5}$ (3.96×10^{-5})
$\sigma = 2.05 \times 10^{-6}$	$\sigma = 2.08 \times 10^{-6}$
Spectral range = 1.179 ppm	Spectral range = 1.206 ppm
Number of data points = 45	Number of data points = 46

The approximate σ values are given in brackets. The separation between the α- and β-ATP ^{31}P peaks ($\delta_{\alpha\beta}$) is used often for specific information in *in vivo* NMR and in this spectrum we have the result $\delta_{\alpha\beta} = 8.517$ ppm. The σ value is given by $\{(\sigma_3(\alpha\text{-ATP}))^2 + \{(\sigma_3(\beta\text{-ATP}))^2\}^{0.5}$, which is 0.00735 ppm. This gives us the error in the peak separation. To determine the error in the signal separation we need to determine the $\sigma(m_3)$ values for both signals. Using the m_1 values as an approximate measure of the signal height (the S value) and estimating the noise level relative to the signal, we may estimate the SNR for both cases as 8.5 and 12.9 for the α- and β-ATP peaks, respectively. (We note that this spectrum is one of the better spectra, where the SNR is relatively large for this type of work. The noise level was determined from each spectrum by estimating the noise height range, which corresponded to the $2N$ value.) From Eq. [47], we then determine an approximate $\sigma(m_3)$ value for the α-ATP, $\sigma(m_3)_\alpha = 0.0086$ (0.110/12.9). In the β-ATP case we need to take into account the small m_2 value. From Eq. [48], we would obtain $\sigma(m_3)_\beta = 0.0294$ ppm (0.250/8.5). Equation [48], however, has not been tested for such small m_2 values. Hence to check the result of 0.0294 ppm we may derive the appropriate equation by carrying out the interaction of the single noise peak with a signal with $m_2 = 1.04$ ppm^{-2}, as described earlier, obtaining equations similar to Eq. [33]. For the $\sigma(m_3)$ value we obtain $\sigma(m_3) = 0.330(N/S)$. In this case $\sigma(m_3)_\beta = 0.0388$ ppm (0.330/8.5). We shall use this result. The $\sigma(m_3)$ value for $\delta_{\alpha\beta}$ is given by $\{(\sigma(m_3)_\alpha)^2 + \{(\sigma(m_3)_\beta)^2\}^{0.5}$, which is 0.0397 ppm. Hence we estimate that $\delta_{\alpha\beta} = 8.517 \pm 0.079$ ppm ($\pm 2\sigma$). Hence we would expect the $\delta_{\alpha\beta}$ value to lie between approximately 8.44 and 8.60 ppm.

This $\delta_{\alpha\beta}$ result is from the first of a series of nine observations following injury. The nine values (in ppm) are 8.517 (0), 8.518 (0.5), 8.531 (1.0), 8.548 (1.5), 8.565 (2.0), 8.525 (2.5), 8.565 (3.0), 8.541 (3.5), and 8.594 ppm (4.0), where the time in hours after injury is given in brackets. It may be tempting to show a possible small time dependence from a regression analysis. However, the mean $\delta_{\alpha\beta}$ of the nine values yields $\delta_{\alpha\beta} = 8.545$ ppm with a standard deviation of 0.0258 ppm. Our estimate of the expected errors due to noise in the spectrum gives the larger value of 0.0397 ppm and hence we can rule out any time dependence over the 4-h period. All the nine $\delta_{\alpha\beta}$ values lie within the expected range. (Note that the σ value from the particular spectrum is 0.00735 ppm, which is much smaller than the experimental error, $\sigma(m_3)_{\alpha\beta}$, of 0.0258 ppm and even smaller than the estimated $\delta_{\alpha\beta}$ error, $\sigma(m_3)_{\alpha\beta}$, of 0.0308 ppm due to noise in the spectrum.)

The analysis of all the β-ATP peaks yields the results in Tables 11 and 12, assuming Lorentzian and Gaussian lineshapes, respectively. We note that the σ values from the single analysis given above are much smaller than those for the average m_i values given in Table 11. For the Lorentzian case the m_2 value is much less than 10 and hence we shall use Eq.

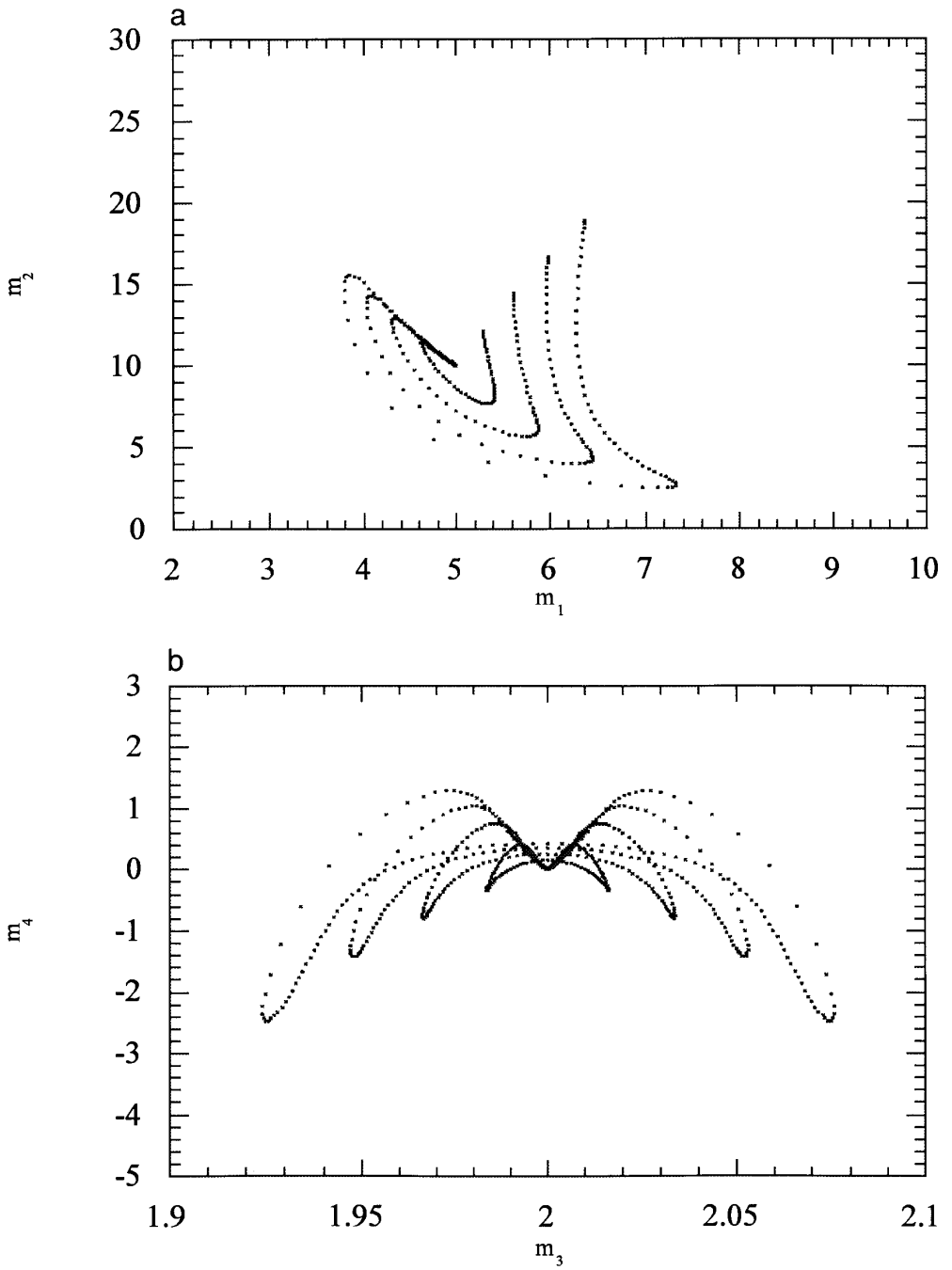

FIG. 8. Two *m* plots for the result of the interaction of a single noise peak on the signal with $sm_1 = 5$, $sm_2 = 10$ ppm^{-2}, $sm_3 = 2$ ppm and $sm_4 = 0$. The height of the noise peak has been chosen as $N = 0.5$, 1.0, 1.5, and 2.0. The shortest contour is when $N = 0.5$ and the longest contour when $N = 2.0$. (a) m_2 versus m_1 and (b) m_4 versus m_3.

[48] to take this into account in determining the $\sigma(m_2)$ and $\sigma(m_3)$ values.

We note from our example that $\sigma(m_3)_\alpha$ and $\sigma(m_3)_\beta$ are similar and we may approximately write $\sigma(m_3)_{\alpha\beta}$, the σ value for the $\delta_{\alpha\beta}$ value, as $\sigma(m_3)_\beta\sqrt{2}$. Using a SNR value of 3 and the mean m_2 value we find that the σ value would be about 0.065. This is larger than the experimentally determined value given in Table 11. Likewise, we estimate, using the mean m_2 value of 3.5 ppm^{-2} and a SNR of 3, that $\sigma(m_2) = 4.05$. For the Gaussian case we estimate an average $\delta_{\alpha\beta}$ value of about 0.040 ppm and a $\sigma(m_2)$ value of approximately 3.34 ppm^{-2}.

We may even simplify such an analysis of results to give a rough estimate of the errors in the $\delta_{\alpha\beta}$ value. This is easy to carry out and is a quick method to give an insight into the magnitude of the likely errors. Here we shall consider only the Lorentzian case. Let us assume that the m_2 value for the β-ATP peak may be about 3.5 ppm^{-2}. Assuming that the α- and β-ATP ^{31}P peaks have the same SNR, then the $\sigma(m_3)_{\alpha\beta}$ may be expressed as $0.163(N/S)$ since for the α-ATP ^{31}P peak $\sigma(m_3) = 0.111(N/S)$ (from Eq. [47]) and for the β-ATP ^{31}P peak $\sigma(m_3) = 0.120(N/S)$ (from a single noise peak analysis). If some of the spectra have SNR = 3, the smallest value we observed, we have the result $\sigma(m_3)_{\alpha\beta} = 0.054$, which is slightly greater than $\sigma(m_3)_{\alpha\beta} = 0.052$ given in Table 11.

Thus, when compared to our estimate of the expected standard deviations, the m_2 and m_3 values of our experimental values strongly suggest that the differences between the 54 experimental *m* values can be easily attributed to errors due to noise in the spectrum. Therefore, any effect due to the brain injury, in this case, must be less than the errors associated with the noise in the spectrum.

CONCLUSIONS

In this paper we have derived simple general formulas with which to determine the standard deviations (the σ_i values) and the correlation matrix elements (the ρ_{ij} values) for the parameters used to define a specific peak in a MRS spectrum. In addition and, more importantly, we have shown how to determine, by several methods, the errors (the $\sigma(m_i)$ values) in these parameters when they are used to estimate a set of parameters to describe the signal within the peak. These errors arise from the effect of complex correlated noise spectra on the signal measurements. We have presented the general form of the $\sigma(m_i)$ values and have shown that they reflect the average noise pattern across the spectrum and not within the vicinity of the peak, as is the case for the σ_i values.

The $\sigma(m_i)$ values may be evaluated by analyzing a large number of simulated spectra. However, we have developed a much quicker method whereby the $\sigma(m_i)$ values may be determined, to a good approximation, by considering the effect of a single noise peak on the signal. This then leads directly to an estimate of the $\sigma(m_i)$ values for a peak from a single MRS spectrum following an estimate of the SNR plus knowledge of the noise standard deviation and the correlation length or, in the terms used in this paper, χ^2_{noise} (ppm^{-1}) and the gap values. Hence our results give a ready means of estimating the error in a particular m_i value from a single MRS spectrum.

Finally, we have illustrated how knowledge of the $\sigma(m_i)$ values may be used to readily assess the significance of a set of experimental results derived from *in vivo* ^{13}P MRS spectra. What has emerged from this work is the knowledge that the errors in determining the signal parameter in a spectrum with correlated noise, where the SNR is small, are much larger than expected and cannot be ignored. Thus as this situation is observed frequently in ^{31}P *in vivo* MRS our work demonstrates that any interpretation, for example, of the chemical shift difference between the α- and β-^{31}P in ATP is most likely meaningless unless it is coupled with a careful assessment of the likely errors. In such papers it should be mandatory to use a statistically precise method in determining the signal parameters and a reliable estimate of the errors due to the correlated noise.

TABLE 11
The Results of Fitting the ^{31}P β-ATP Peak to a Lorentzian Lineshape

Value	m_1	m_2	$\delta_{\alpha\beta}$	m_4
Minimum	3.71*e*-05	1.07	8.474	−2.37*e*-05
Maximum	1.41*e*-04	17.22	8.716	8.55*e*-04
Mean	8.20*e*-05	3.50	8.581	3.14*e*-04
$\sigma(m_i)$	2.32*e*-05	2.42	0.05238	2.52*e*-05
Spectra	54	54	54	54

TABLE 12
The Results of Fitting the ^{31}P α-ATP Peak to a Gaussian Lineshape

Value	m_1	m_2	$\delta_{\alpha\beta}$	m_4
Minimum	2.57*e*-05	2.23	8.473	1.13*e*-05
Maximum	9.00*e*-05	22.73	8.717	1.02*e*-04
Mean	5.29*e*-05	6.94	8.580	6.02*e*-05
$\sigma(m_i)$	1.51*e*-05	3.37	0.05246	2.25*e*-05
Spectra	54	54	54	54

ACKNOWLEDGMENTS

This research was initiated to more fully understand earlier work undertaken at James Cook University of North Queensland in the study of *in vivo* measurements from ^{31}P MRS spectra. E. M. Golding acknowledges the strong support and encouragement from Dr. Geoffrey P. Dobson during this time. In addition, the authors express their sincere gratitude to the reviewer for his/her valuable comments, which have resulted in a more generalized approach to the method that we have developed for estimating the errors in the signal parameters where the noise is significant and correlated.

REFERENCES

1. D. G. Gadian, "Nuclear Magnetic resonance and Its Applications to Living Systems," Oxford Univ. Press, Oxford (1982).
2. E. M. Golding, G. P. Dobson, and R. M. Golding, A critical assessment of noise-induced errors in ^{31}P MRS: Application to the measurement of free intracellular magnesium *in vivo, Magn. Reson. Med.* **35,** 174–185 (1996).
3. R. Vink, T. K. McIntosh, P. Demediuk, M. W. Weiner, and A. I.

Faden, Decline in intracellular free magnesium concentration is associated with irreversible tissue injury following brain trauma, *J. Biol. Chem.* **263,** 757–761 (1988).

4. D. W. Posener, Precision in measuring resonance spectra, *J. Magn. Reson.* **14,** 121–128 (1974).
5. L. Chen, C. E. Cottrell, and A. G. Marshall, Effect of signal-to-noise ratio and number of data points upon precision in measurement of peak amplitude, position and width in Fourier transform spectrometry, *Chem. Int. Lab. Syst.* **1,** 51–58 (1986).
6. R. R. Ernst, Advances in magnetic resonance, *in* "Sensitivity Enhancement in Magnetic Resonance" (J. S. Waugh, Ed.), Vol. 2, pp. 1–135, Academic Press, New York (1966).
7. J. S. Ingwall, Phosphorus nuclear magnetic resonance spectroscopy of cardiac and skeletal muscles, *Am. J. Physiol.* **242,** H729–H744 (1982).
8. A. A. Maudsley, Spectral lineshape determination by self-deconvolution, *J. Magn. Reson.* **106,** 47–57 (1995).
9. D. Shaw, "Fourier Transform NMR Spectroscopy," Elsevier, Amsterdam (1976).
10. W. C. Hamilton, "Statistics in Physical Science," Ronald Press, New York (1964).
11. W. H. Press, W. T. Vetterling, S. A. Teukolsky, and B. P. Flannery, "Numerical Recipes in C," 2nd ed., Cambridge Univ. Press, New York (1992).
12. M. B. Priestley, "Spectral Analysis and Time Series," Academic Press, London (1981).